

PULSE DELAYS AND GAIN CHARACTERISTICS IN  
TEA CO<sub>2</sub> LASERS

PULSE DELAYS AND GAIN CHARACTERISTICS IN  
TEA CO<sub>2</sub> LASERS

By

JOHN REID, B.A. (Oxon.)

A Thesis

Submitted to the Faculty of Graduate Studies  
in Partial Fulfilment of the Requirements  
for the Degree  
Master of Science.

McMaster University

March 1972

MASTER OF SCIENCE (1972)  
(Physics)

McMASTER UNIVERSITY  
Hamilton, Ontario.

TITLE: Pulse Delays and Gain Characteristics in TEA  
CO<sub>2</sub> Lasers

AUTHOR: John Reid, B.A. (Oxford University)

SUPERVISORS: Dr. B. K. Garside and Dr. E. A. Ballik

NUMBER OF PAGES: 90, vii

SCOPE AND CONTENTS: A novel method is reported for studying the time-dependent gain and cavity losses in a TEA CO<sub>2</sub> laser. The technique involves an investigation of the time delay of the onset of lasing with respect to the current pulse in such a laser. Detailed measurements of this time delay as both the laser gain and the cavity loss are varied, in conjunction with a simple theoretical analysis, permit the evaluation of parameters describing the time-dependent gain and the cavity loss. A refinement of the technique, using two amplifier tubes, allows an accurate measurement of the decay time of the gain.

## ACKNOWLEDGEMENTS

The author is indebted to Dr. B. K. Garside and Dr. E. A. Ballik for providing the impetus for this study, and for their encouragement and helpful suggestions during the course of its execution.

To all who were involved in the manufacture of the apparatus, especially in the machine shop, I express my appreciation.

I am indebted to McMaster University for its support during the time of this project, in the form of a Teaching Assistantship.

This work was supported in part by the Defence Research Board of Canada.



## TABLE OF CONTENTS

	PAGE
CHAPTER I: INTRODUCTION	1
1.1 The TEA CO <sub>2</sub> Laser	1
1.2 Scope of This Thesis	2
CHAPTER II: A MODEL FOR THE TIME-DEPENDENT GAIN AND THE LASER PULSE BUILD-UP TIME	5
2.1 A Model for the Time-Dependent Gain	6
2.2 Laser Pulse Build-Up	10
CHAPTER III: EXPERIMENTAL APPARATUS AND PROCEDURE	12
3.1 The Electrical System	14
3.2 The Optical System	17
3.3 The Detection System	24
3.4 Current and Voltage Probes	29
3.5 Alignment Procedure	33
3.6 Measurement of Pulse Delays	34
CHAPTER IV: EXPERIMENTAL RESULTS AND DISCUSSION	37
4.1 Current Pulses	37
4.2 Laser Pulse Delays	44
4.3 Contact between Theory and Experiment	49
4.4 Results and Discussion	51

	PAGE
CHAPTER V: A MORE ACCURATE MEASUREMENT OF $T_2$ USING AN ADDITIONAL GAIN TUBE	55
5.1 Theory	56
5.2 Experimental Arrangement	59
5.3 Experimental Observations and Discussions	62
CHAPTER VI: CONCLUSIONS AND RECOMMENDATIONS	68
APPENDIX I: POLISHING METHOD FOR NaCl	72
APPENDIX II: DATA	74
REFERENCES	88

## LIST OF ILLUSTRATIONS

FIGURE		PAGE
2-1	Typical variation of gain with time	9
3-1	Photographs of the entire apparatus	13
3-2	Discharge circuit	16
3-3	Close-up photograph of the helical resistor structure	20
3-4	Photograph of the end-window units	21
3-5	Relation of the inserted cavity loss to the angle turned by the two NaCl discs	22
3-6	Photograph of the variable loss unit	23
3-7	Diagram of the simple detection circuit	26
3-8	Photograph of the detection sub-system	27
3-9	Schematic diagram of the entire laser system	28
3-10	Diagram of the current probe	30
3-11	Diagram of the voltage probe	31
3-12	Typical current and voltage pulses	32
3-13	Typical oscilloscope traces from which $t_d$ is measured	36
4-1	Variation of the time-integrated current pulse with the capacitor charging voltage $V_c$	42
4-2	Plots of the current pulse widths	43

FIGURE		PAGE
4-3	The time delay ( $t_d$ ) of the onset of lasing with respect to the peak of the current pulse as a function of normalised voltage	46
4-4	The time delay ( $t_d$ ) as a function of normalised voltage for a different gas mixture	47
4-5	Plots of the time delay of the onset of lasing with respect to the current pulse peak, against normalised voltage for several values of the cavity loss	48
5-1	Schematic diagram of two-amplifier apparatus	60
5-2	Variation of time delay ( $t_d$ ) with charging voltage	61
5-3	Fall-time of time-dependent gain	66
5-4	Fall-time of time-dependent gain; nitrogen-containing gas mixture	67

## CHAPTER I

### INTRODUCTION

#### 1.1 The TEA CO<sub>2</sub> Laser

Laser action at 10.6  $\mu\text{m}$  in a CO<sub>2</sub>-N<sub>2</sub>-He gas mixture at atmospheric pressure was first reported by Beaulieu <sup>(1)</sup> in 1970. The gas mixture was excited by fast electrical discharges transverse to the laser axis; hence the name TEA lasers (Transversely Excited Atmospheric pressure). The laser action is similar to that of low pressure CO<sub>2</sub> lasers, but the increased pressure leads to much higher output intensities in pulsed operation. Much work <sup>(2-5)</sup> was carried out to find high-efficiency electrode configurations. Both spark and volume discharges were examined. One electrode configuration, a double helix <sup>(6)</sup>, has the advantage of a mode-selecting effect, which tends to give laser action in the fundamental mode only. This configuration was used throughout the work described in this thesis; the helical construction is described in detail in Section 3.4. For further information concerning TEA CO<sub>2</sub> lasers, the reader is referred to the list of references cited, and in particular to the review article by Beaulieu <sup>(7)</sup>.

## 1.2 Scope of This Thesis

An investigation is reported of the time delay of the onset of lasing, with respect to the discharge current pulse, in TEA CO<sub>2</sub> lasers. Detailed measurements of the variation in this delay as a function of both the laser gain and the cavity loss have been made for certain gas mixtures. The data so obtained have been related to a simple theory for the build-up of the laser pulse energy in the cavity, coupled with a simple model for the time-dependent gain. For the most part, detailed analysis has been restricted to gas mixtures not containing nitrogen. CO<sub>2</sub>: He mixtures give slightly more stable operating conditions, and avoid the problem of N<sub>2</sub>-CO<sub>2</sub> energy transfer processes (8). However, a preliminary investigation of nitrogen-containing gas mixtures indicates that a similar analysis is appropriate to this case also. The application of the theoretical model to experimental observations permits the evaluation of parameters describing the time-dependent gain and the laser cavity losses. Optimisation of the fit between theory and experiment allows good values to be obtained for the peak gain, the risetime and the decay time of the gain, and the average cavity loss per pass. This work is reported in Chapters 2, 3 and 4. Chapter 5 deals with a refinement of the technique to measure more accurately the decay time of the

gain. The parameters obtained in this way are in good agreement with other reported data, where available. The work reported in this thesis is summarised in two papers by Garside et al. (9), Reid et al. (10).

A number of authors (11-14) have reported the use of CW low pressure CO<sub>2</sub> lasers to probe the gain of a TEA CO<sub>2</sub> laser amplifier directly, using a simple single-pass technique. This technique has the advantage of being both direct and conceptually simple. However, it also suffers certain disadvantages. A major problem is the necessity of measuring rather small signals in the presence of large radio-frequency noise due to switching transients in the laser discharge process. The need to detect relatively small intensity changes in the presence of this noise renders the technique somewhat insensitive, and enforces the use of rather sophisticated experimental techniques. In addition, time-dependent refractive index effects in the amplifier tend to deviate the probing laser beam (11), thereby causing erroneous changes in detected intensity, and providing a potential source of error in the measured decay time. Finally, great care must be taken in such measurements to avoid influencing the results by allowing extraneous TEA CO<sub>2</sub> discharge light to fall on the detector (15).

The method described in this thesis for obtaining information concerning the time-dependent gain and the cavity loss is attractive since no elaborate experimental



techniques are involved. Furthermore, since the observations are made on the high intensity lasing output, the results are not plagued by the radio-frequency pick-up problems involved in direct gain measurements. In addition, since it is only necessary to make measurements of time delays, the need to compare intensities is obviated.

An understanding of the gain mechanism in TEA CO<sub>2</sub> lasers provides important information concerning the behaviour of the time-varying population inversion in the amplifier tube. Such information permits the adjustment of the medium composition and discharge characteristics to generate optimised laser systems. In addition, a knowledge of the time-variation of the gain provides considerable insight into the relative importance of the many excitation and de-excitation processes which can occur in the atmospheric pressure discharges of TEA CO<sub>2</sub> amplifiers.



## CHAPTER II

### A MODEL FOR THE TIME-DEPENDENT GAIN AND THE LASER PULSE BUILD-UP TIME

The theory of pulse delays in TEA CO<sub>2</sub> lasers is presented in two sections. Firstly, a simple model is assumed which describes the time-dependent gain present in the laser cavity immediately after the discharge current pulse. Secondly, a simple theory describes the build-up, from the noise level, of the laser pulse energy in the cavity, under the action of this time-dependent gain. The time after the start of the gain build-up for a significant energy density to appear in the laser cavity can be calculated, and compared with experimental data. Details of the theory are given below.

## 2.1 A Model for the Time-Dependent Gain

It is supposed that the upper and lower laser levels are equally excited by the discharge current, and the inversion comes about through the subsequent decay of both laser levels. Only the vibrational levels of the system are considered, the rotational sub-structure is not considered since the rotational levels associated with each vibrational level are strongly coupled. The validity of the various approximations employed in this calculation are discussed elsewhere (16,17). Furthermore, the parametrisation of the gain, in terms of two exponentials, is of more general validity than indicated above. Indeed, it has been found to describe experiment to a good approximation even for gas mixtures containing nitrogen.

The upper and lower laser level populations,  $N_2$  and  $N_1$  respectively, are assumed to obey the following equations:

$$\frac{dN_2}{dt} = -\frac{N_2}{T_2} + R_2 I(t) \quad (2-1)$$

$$\frac{dN_1}{dt} = -\frac{N_1}{T_1} + R_1 I(t) \quad (2-2)$$

where  $I(t)$  is the discharge current pulse and  $R_1$ ,  $R_2$  are excitation rates employing appropriately averaged cross-sections,

$T_2$  and  $T_1$  are the lifetimes of the upper and lower laser vibrational levels. Since the initial inversion is taken to be negligible with respect to that subsequently appearing, it is supposed that  $R_1 = R_2 = R$ . Equation (2-1) has a formal solution given by:

$$N_2(t) = R_0 e^{-t/T_2} \int_0^t [e^{t'/T_2}] I(t') dt' \quad (2-3)$$

and equation (2-2) has a solution of the same form.

In general, it is assumed that the laser discharge current pulses are short compared with both the observed laser pulse delays and also  $T_1$ . It is not particularly difficult to relax this requirement, but it is both experimentally and theoretically convenient to retain it. For certain ranges of experimental (discharge and laser cavity) parameters, the above approximation is poor, and so some care must be taken to exclude these regions in the comparison between theory and experiment. This procedure is described fully in Section 4.1. The restriction to very short current pulses allows the theory to be simplified still further. The solution for  $N_2$  becomes;

$$N_2(t) = R_0 e^{-t/T_2} \int_0^t I(t') dt' \quad (2-4)$$

Now, let:  $N_0 = R_0 \int_0^t I(t') dt'$

then

$$N_2(t) - N_1(t) = N_0 (e^{-t/T_2} - e^{-t/T_1}) \quad . \quad (2-5)$$

Now, since the gain ( $g$ ) is proportional to the population inversion, it can be written as:

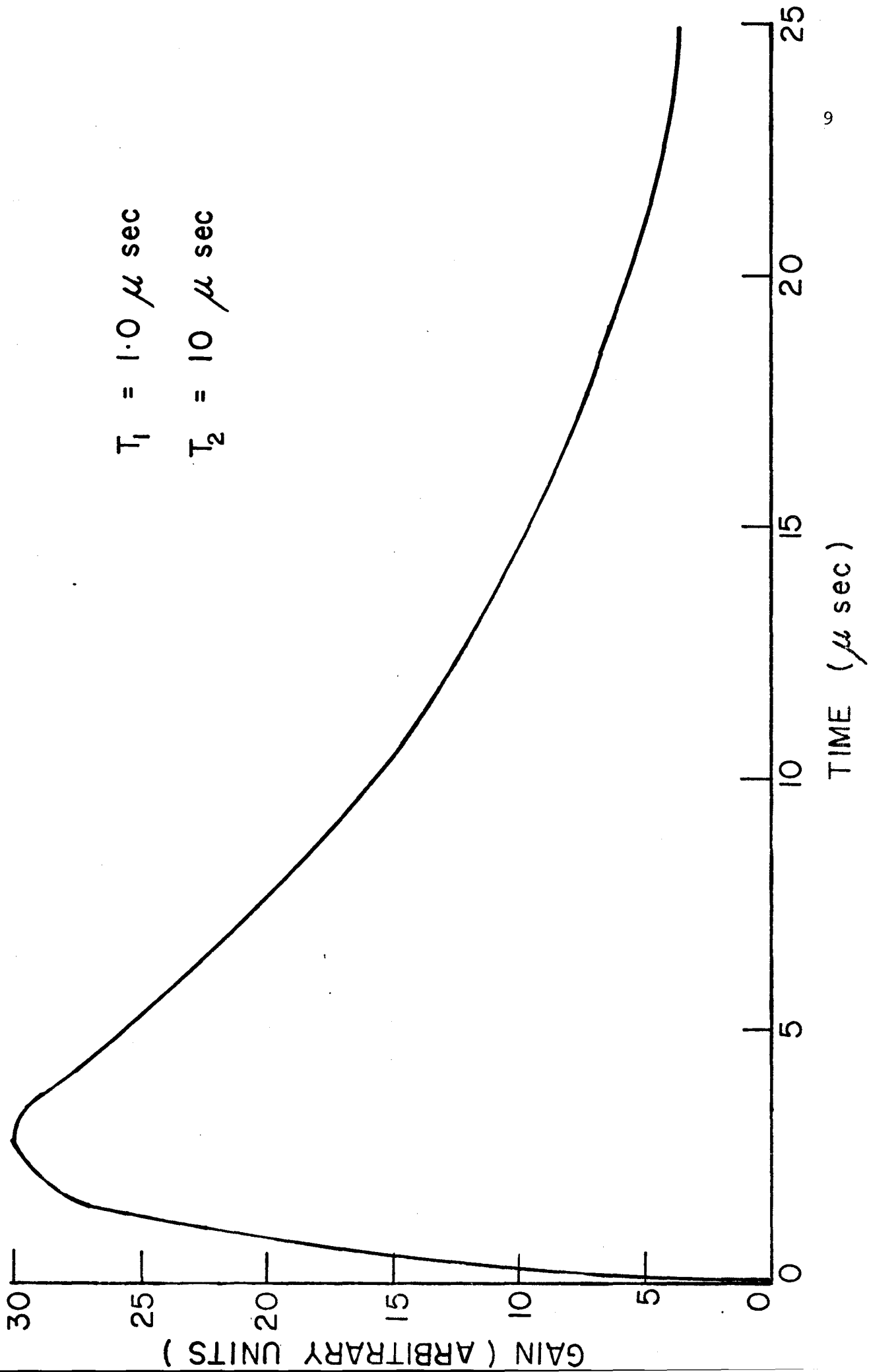
$$g(t) = g_0 (e^{-t/T_2} - e^{-t/T_1}) \quad . \quad (2-6)$$

This expression for gain is used throughout the rest of this thesis, the values of  $g_0$ ,  $T_2$  and  $T_1$  being varied to suit the experimental and theoretical conditions. This form for the time-dependent gain is appropriate for the situation in which the upper and lower laser levels are equally excited at  $t = 0$ , and the inversion is produced by the subsequent decay of the laser levels. Direct measurements of the time-dependent gain by Robinson (11,12) have indicated that the above form for the gain is appropriate for a number of typical gas mixtures.

Typical values for  $T_1$  and  $T_2$  are 1  $\mu$ s and 10  $\mu$ s respectively. Figure (2-1) shows the variation of gain with time for these values of  $T_1$  and  $T_2$ .

Figure (2-1)

Typical variation of gain with time



## 2.2 Laser Pulse Build-Up

The radiation density in the laser cavity,  $\rho$ , must satisfy the following equation:

$$\frac{d\rho}{dt} = \rho g'(t) - \rho/\tau_c \quad (2-7)$$

where  $\tau_c$  is the lifetime of the radiation in the laser cavity, and  $g'(t)$  is the gain in appropriate units. The above equation can be solved when the gain is supposed to vary as in equation (2-6), but gain saturation effects are ignored. The solution is:

$$\ln(\rho_f/\rho_i) = \int_{t_{th}}^{t_f} [g'(t) - 1/\tau_c] dt \quad (2-8)$$

where, when  $t = t_{th}$ ,  $g'(t_{th}) = 1/\tau_c$ . Physically, this means the energy density in the cavity only begins to build-up rapidly once the gain becomes greater than the loss (i.e., after  $t = t_{th}$ ). The integral can be carried out directly, yielding, after some rearrangement:

$$\begin{aligned} \ln(\rho_f/\rho_i) = & g'_0 e^{-t_{th}/T_2} [T_2(1 - e^{-t_f/T_2}) - t_f] \\ & - g'_0 e^{-t_{th}/T_1} [T_1(1 - e^{-t_f/T_1}) - t_f] \quad (2-9) \end{aligned}$$

where  $\rho_f$  and  $\rho_i$  are the initial and final radiation densities, and  $t_f$  is the time taken to reach  $\rho_f$ , measured from  $t_{th}$ .

This equation, together with the subsidiary equation for  $t_{th}$ :

$$1/\tau_c = g'_0 (e^{-t_{th}/T_2} - e^{-t_{th}/T_1}) \quad (2-10)$$

determines the value of the time-delay, with respect to the current pulse, of the build-up of the radiation from  $\rho_i$  to  $\rho_f$ .

The laser pulse build-up theory uses expression (2-6) for the low signal gain. Saturation effects are neglected. Consequently, it only applies provided the laser intensity has not built-up to a level sufficient to produce significant gain saturation. The experimental procedure used to ensure this is described in Section 3.6.



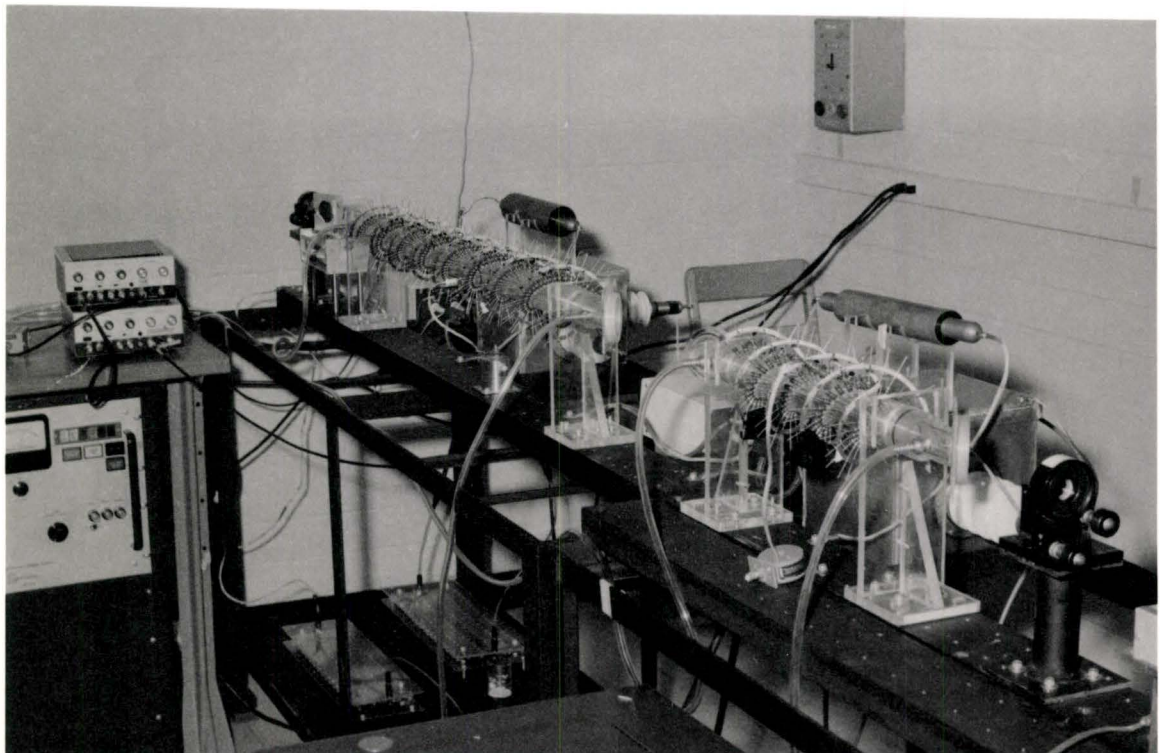
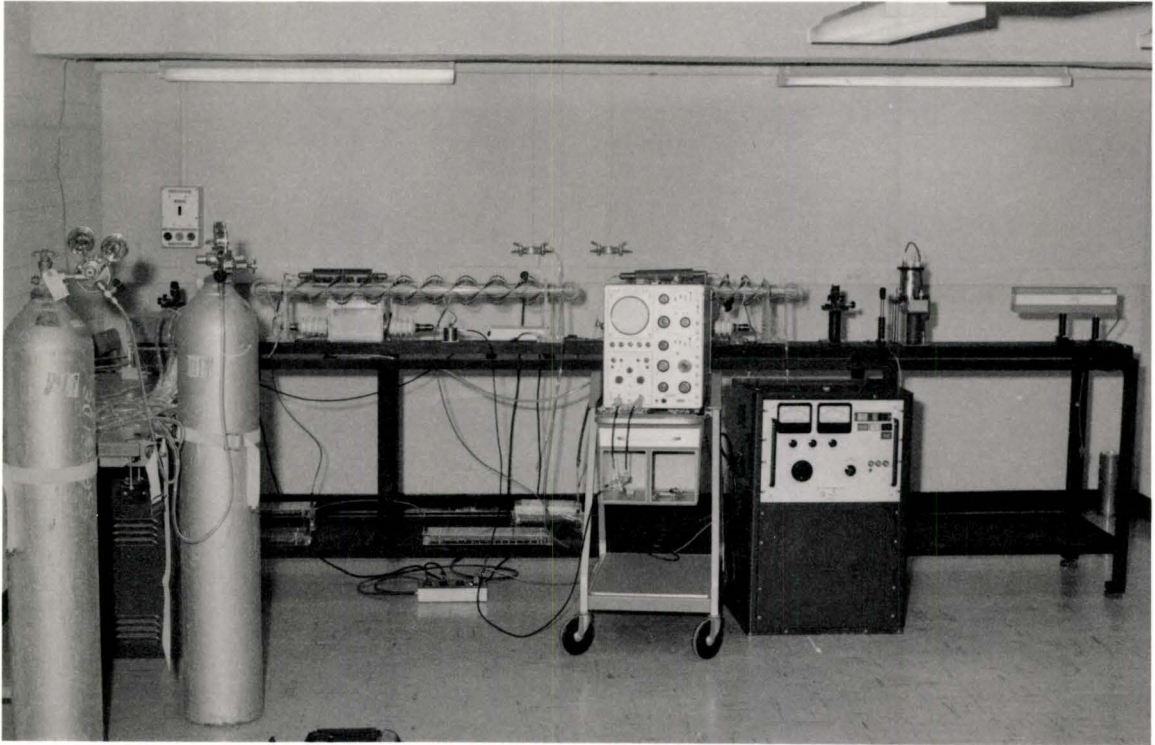
## CHAPTER III

### EXPERIMENTAL APPARATUS AND PROCEDURE

This description of the experimental apparatus is divided into several sections. The first section deals with the electrical circuit which delivers the current pulse to the laser tube. The next section is entitled "The Optical System", and deals with the laser cavity itself, and the gas flow system. Finally, there are two short sections dealing with the detection system for the laser pulse, and the probes used to measure the electrical characteristics of the discharge. Two further sections deal with experimental procedures. Figure (3-1) shows two photographs of the entire apparatus. The photographs show an additional gain tube in the laser cavity. Details of this will be given in Chapter 5.

Figure (3-1)

Photographs of the entire apparatus



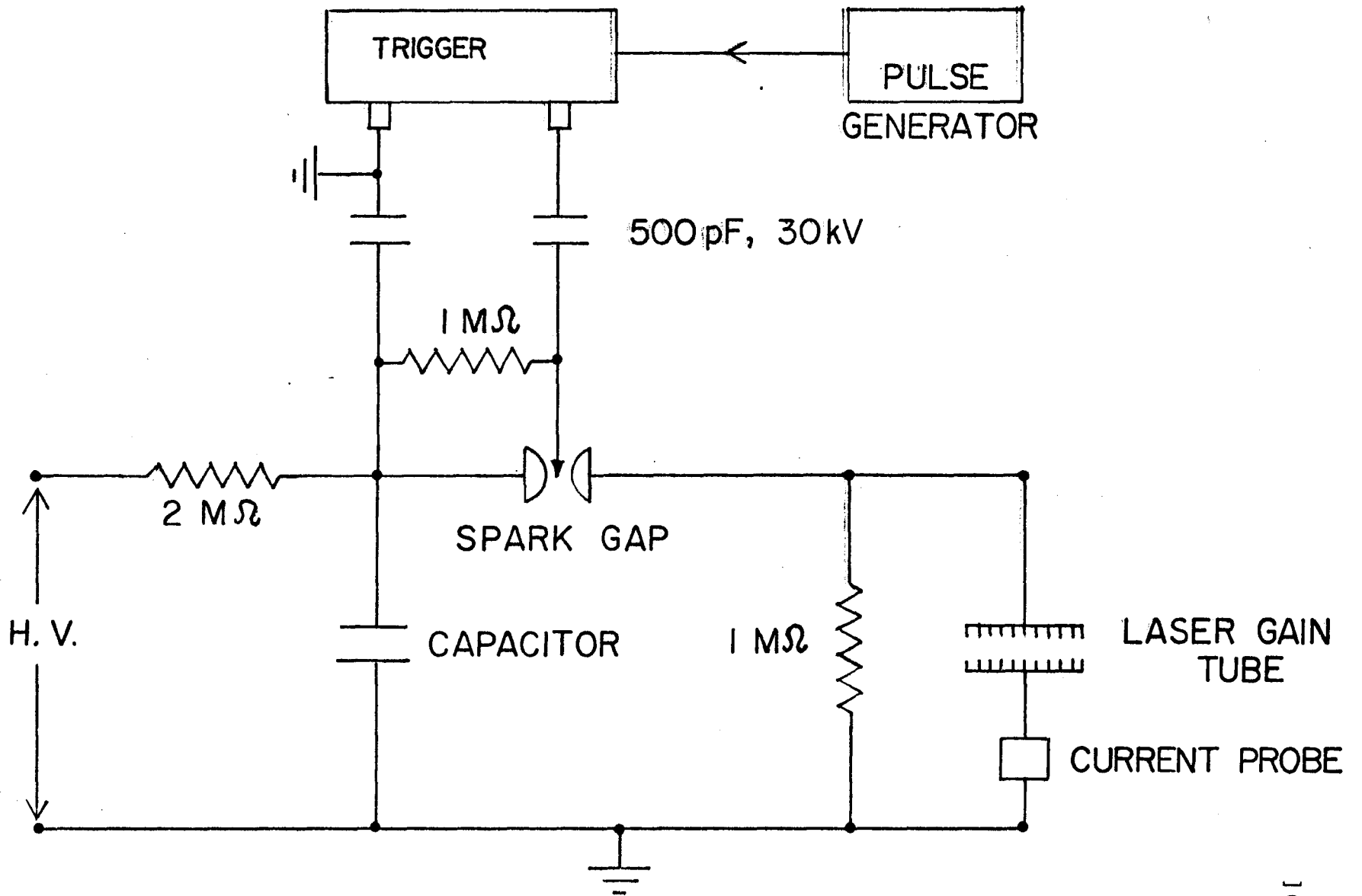
### 3.1 The Electrical System

The electrical circuit used is typical of TEA laser systems. Details of other circuits are given elsewhere (2,6). The circuit essentially consists of a high voltage capacitor which is discharged through the laser tube by means of a triggered spark-gap. The circuit is shown in Figure (3-2) and described in detail below.

The power supply (Universal Voltronics BAL-50-16) can supply 16 mA current at a maximum voltage of 50 kV. The present circuit is limited to 30 kV, and 16 mA is more than adequate for the repetition rates used. The spark-gap (E.G. and G., G.P. 14-B) is oil-immersed and is triggered by an E.G. and G. high voltage Trigger Module (T.M. 11). It is this Module which is limited to maximum hold-off voltage of 30 kV. The Trigger Module is fired by a pulse generator (Data-Pulse 100 A). The 2 M $\Omega$  charging resistor, and 1 M $\Omega$  laser shunt resistor are both made from chains of 100, 1-watt carbon resistors. This avoids the use of expensive high-voltage, large wattage resistors. The capacitors used in the experiments were all rated to 50 kV, and varied in value from 0.001  $\mu$ F to 0.02  $\mu$ F. The charging voltage was varied from the maximum of 30 kV down to the breakdown voltage of the laser tube, approximately 12 kV. The pulse repetition rate was of the order 3 to 5 pulses per second.

In building the circuit, care was taken to avoid the presence of sharp points and corners, and also to provide adequate air insulation for all high voltage apparatus. Even on the most humid days, corona was not a problem, but if the apparatus is to be used above 30 kV, additional precautions may be necessary. All connections were made as short as possible, and thick copper braid was used to reduce the inductance of the discharge circuit. For safety reasons, all high voltage apparatus was placed where it could not be accidentally touched or fallen upon. The capacitor was discharged by a safety relay which closed whenever the power supply was switched off.

Figure (3-2)  
Discharge Circuit



### 3.2 The Optical System

The laser cavity is formed by two germanium mirrors, one plane and one 10 M concave. The plane mirror is coated for maximum reflection, and the 10 M mirror is coated for a reflectivity of 98%, and antireflection coated on the back face. Both mirrors are 1 inch in diameter. The separation of the mirrors was 157 cm, and the cavity contained the laser gain tube, and a NaCl variable loss. Both these will be described presently. A different experimental arrangement is described in Chapter 5.

The laser gain tubes employed are helical structures of a standard type <sup>(6)</sup> employing 1 k $\Omega$  resistors to distribute the current. The tubes themselves are perspex, 2 inches O.D. and 1.5 inches I.D. The anode and cathode resistors (2.7  $\Omega$  and 1 K $\Omega$  respectively) are cut to size and sealed into holes in the tube using an adhesive made from perspex shavings and chloroform. Each resistor is then soldered to a continuous length of tinned, copper braid wound in a helix around the tube. The helices have a pitch of 9 inches; each helix consists of 36 discharges. The tube lengths are 36 inches and the separation of each anode and cathode is 1 inch. A close-up photograph of the tube and resistors is shown in Figure (3-3). The ends of the tubes are sealed by NaCl discs set at Brewster's angle (56°). The units holding the discs are



removable, can be rotated on their O - ring seals, and also contain the gas inlet or outlet connectors. Figure (3-4) is a photograph of one of these units. The tube and its end windows are not vacuum-tight, but as the apparatus is only used at atmospheric pressure, the seal is adequate.

The variable loss also present in the laser cavity consists of two NaCl discs inclined at equal angles to the laser resonator axis and mounted so that they may be rotated through equal angles in opposite senses. This type of mounting is employed so that optical alignment of the laser is not lost as the discs are rotated. The loss introduced into the laser cavity by this element is a known function of the angle of incidence of the laser light on the discs. The loss is effectively zero when both discs are set at Brewster's angle, and increases as the angle becomes greater than Brewster's angle. Figure (3-5) shows a plot of loss against angle, as measured from Brewster's angle. Figure (3-6) is a photograph of the variable loss unit. It was designed to minimise backlash, and the angle rotated can be measured to  $0.1^\circ$  without difficulty. A similar technique has been applied previously in He-Ne lasers (18).

The NaCl discs used in this apparatus were stored in desiccators to protect them from moisture. However, while in use the surfaces were affected by high humidity, and they occasionally had to be repolished. A successful technique was developed and is described briefly in Appendix I.

The laser is operated using a mixture of helium, carbon dioxide and sometimes nitrogen flowing through the gain tube. Cylinders of high purity gases were obtained from Matheson and the flow rates controlled by two-stage regulators, and monitored using Matheson flow-meter tubes, No. 603 for Helium and No. 602 for carbon dioxide and nitrogen. All connections use 1/4 inch plastic tubing, and the waste gas is allowed to flow into the laboratory air. Although several different gas mixtures were used during the experiments, the total flow rate remained constant at 2.3 litres per minute.

Figure (3-3)

A close-up photograph of the helical resistor structure

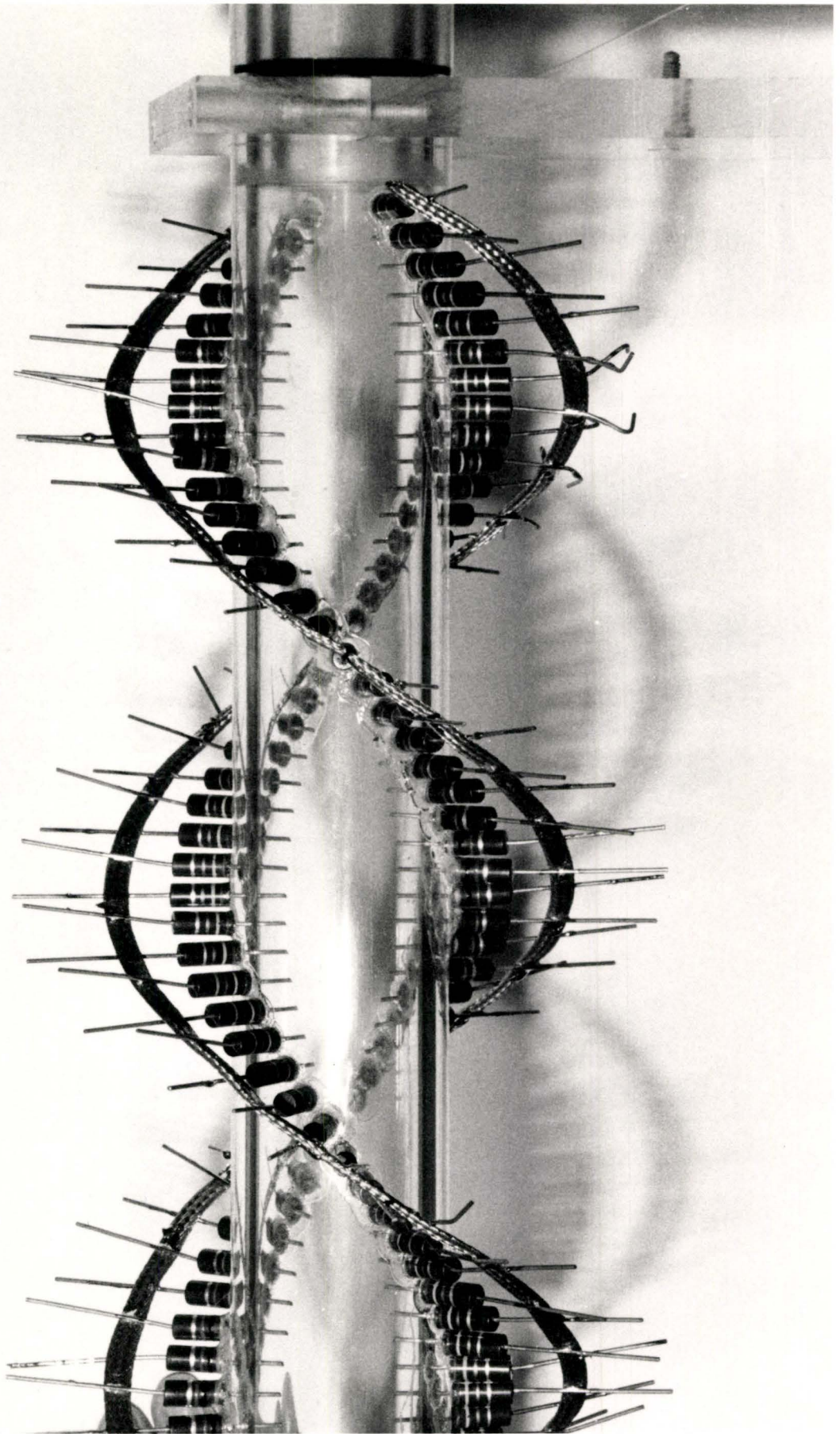


Figure (3-4)

Photograph of the end-window units

Note the O - ring which fits inside the laser tube.  
The NaCl disc is clamped down upon a second O - ring to  
provide a gas-tight seal.



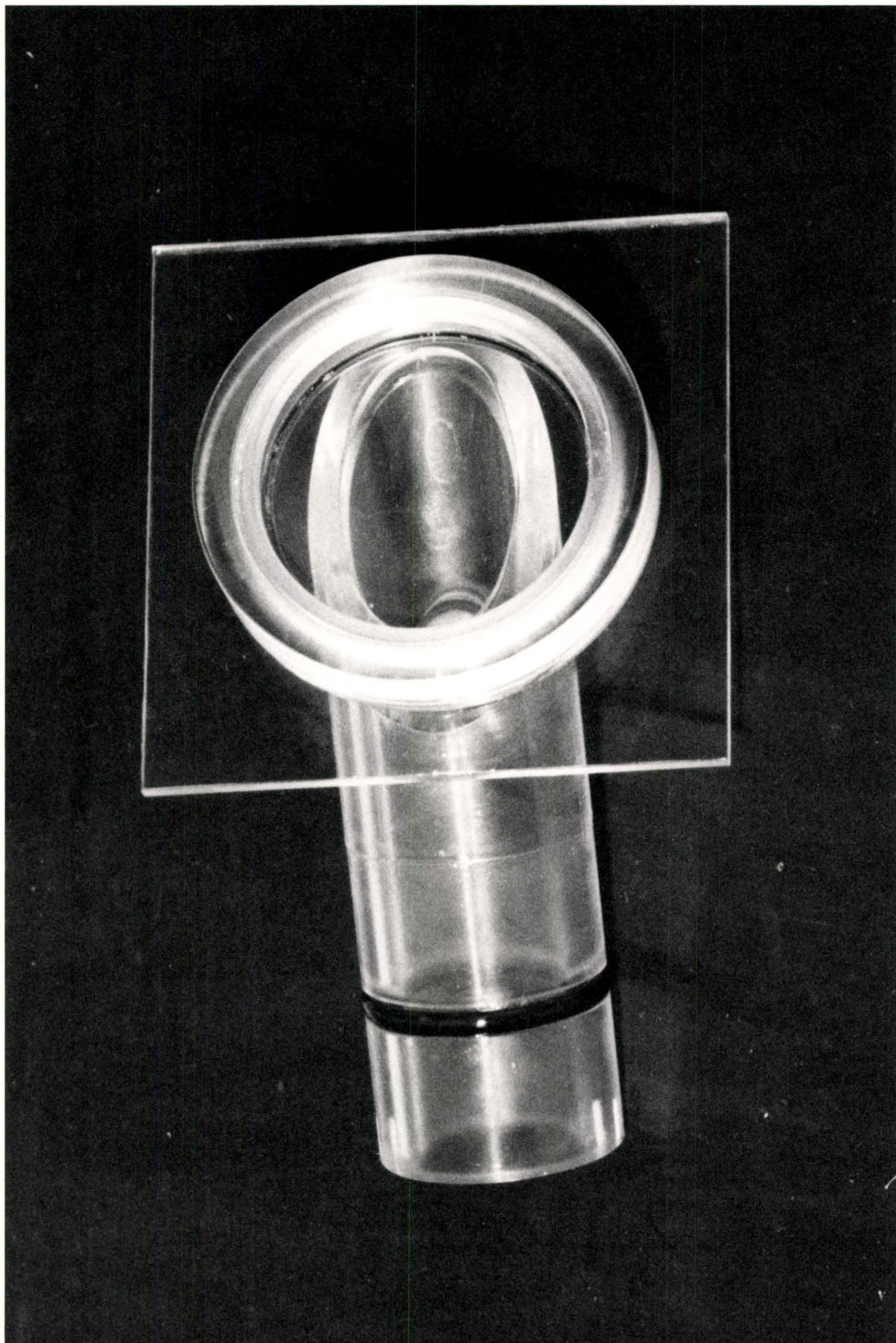


Figure (3-5)

Relation of the inserted cavity loss to the angle turned  
by the two NaCl discs

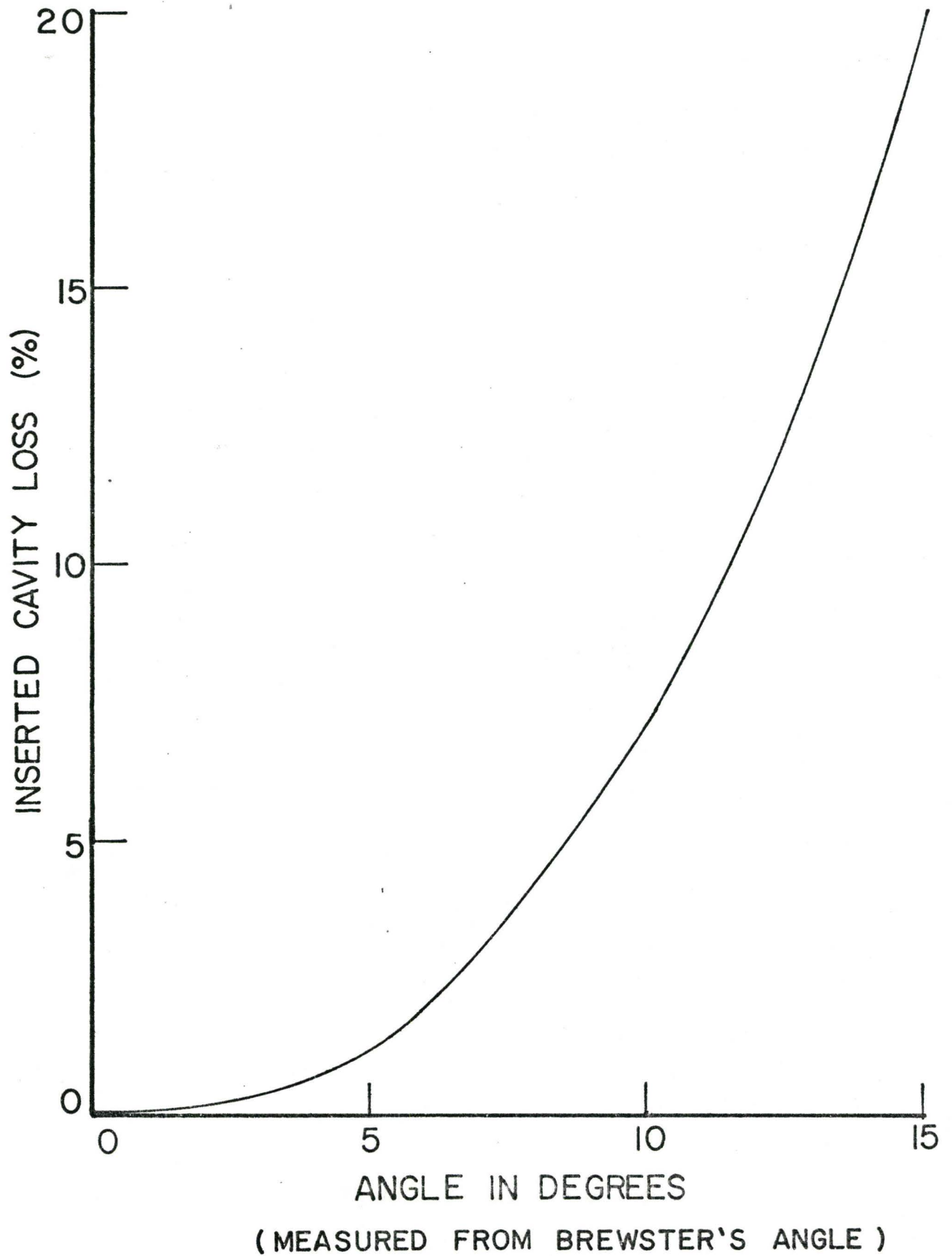
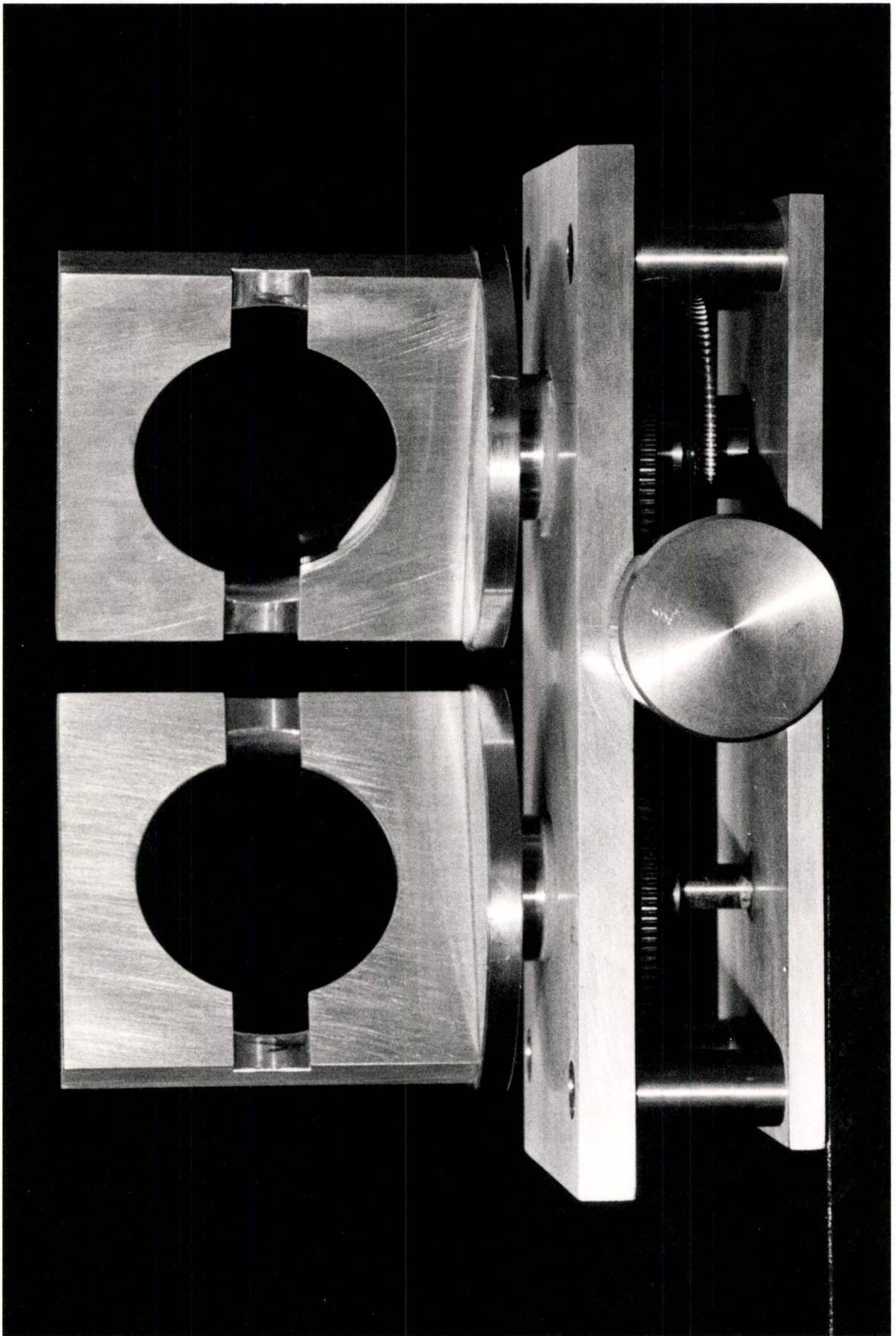




Figure (3-6)

Photograph of the variable loss unit



### 3.3 The Detection System

The radiation output of the TEA CO<sub>2</sub> laser has a wavelength of 10.6  $\mu$ . Special detectors must be used if a fast response time is to be obtained. Two types of detectors were used in this series of experiments. The first was a "photon-drag" type made from 10  $\Omega$ -cm doped germanium (19). This had a very fast response time, could be operated at room temperature, but gave a very small signal (typically 10 mV). The other detector was a commercial gold-doped germanium detector (SBRC-40742) operated at liquid nitrogen temperature. This is a photo-conductive device, and a large signal could be easily obtained. For this reason, the gold-doped germanium detector was used for all measurements. When the laser pulse is examined using a very fast oscilloscope (Hewlett-Packard 183 A, 500 MHz bandwidth) a modulated pulse is observed, the modulation spikes having a time scale of order 10 nanoseconds (20,21). However, as it is only the time to the onset of lasing which is required, the modulation becomes a nuisance. When a Tektronix 547 oscilloscope is used, the modulation is integrated out, but the rise-time of the laser pulse is unaffected. Hence all measurements were made using the Tektronix 547. The simple detection circuit used is shown in Figure (3-7). A short focal-length germanium lens concentrates the laser pulse onto the detector, and

prevents any change in signal due to changes in mirror alignment. A photograph of the entire detection system consisting of lens, Ge: Au detector, and associated circuitry is shown in Figure (3-8). Figure (3-9) is a schematic diagram of the entire laser system.

Figure (3-7)

Diagram of the simple detection circuit

The detector has a "dark" resistance of 6.3 M $\Omega$ .

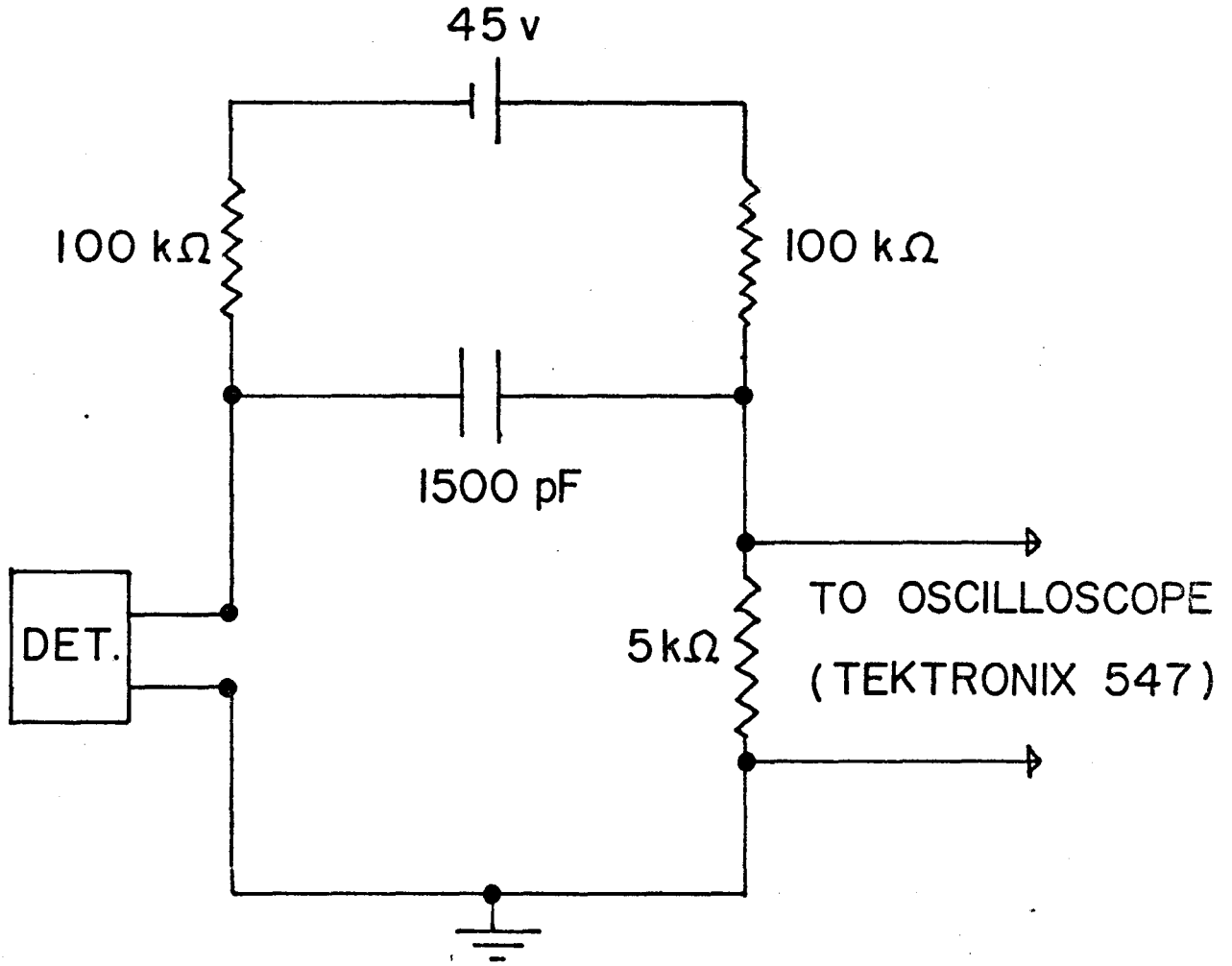


Figure (3-8)

Photograph of the detection sub-system



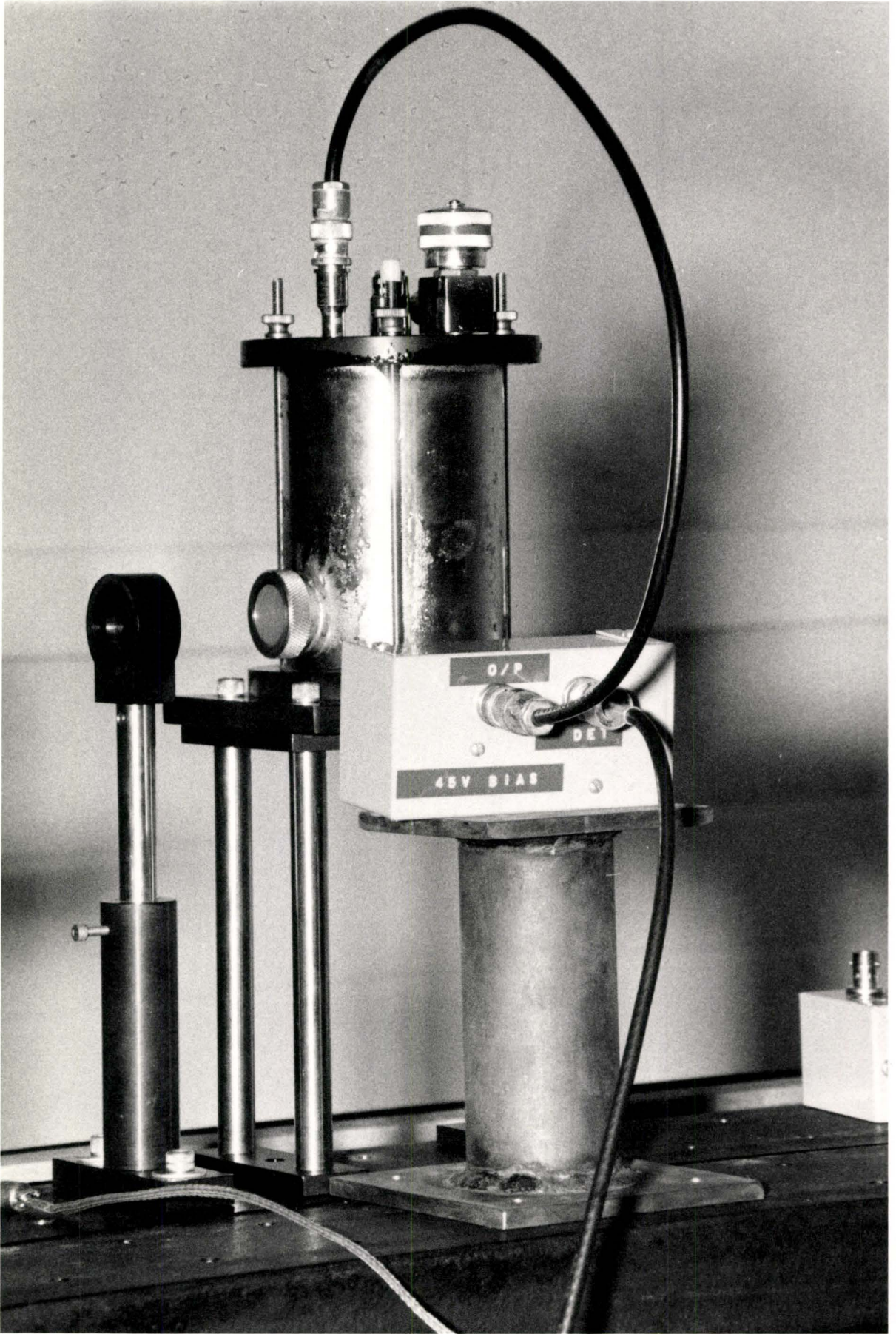
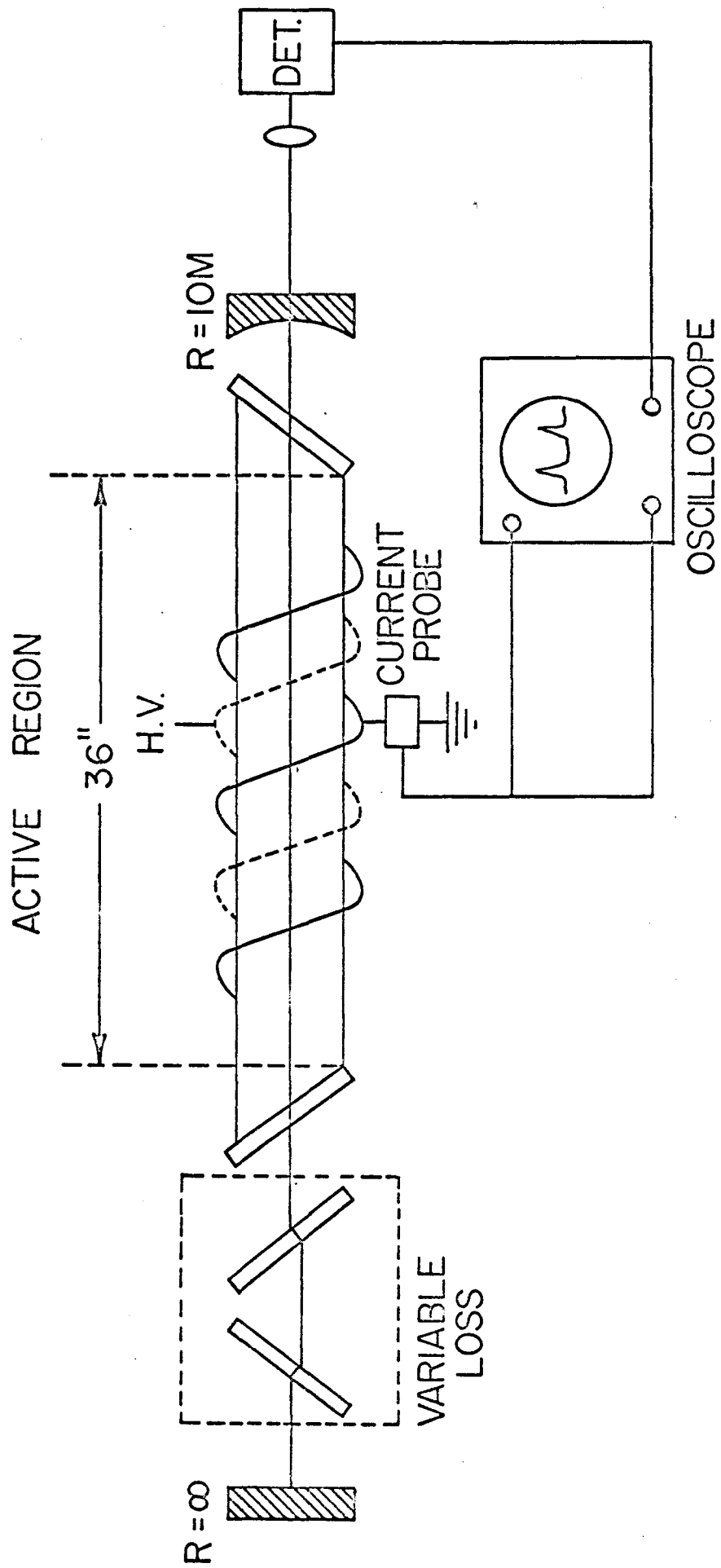




Figure (3-9)

Schematic Diagram of the entire laser system

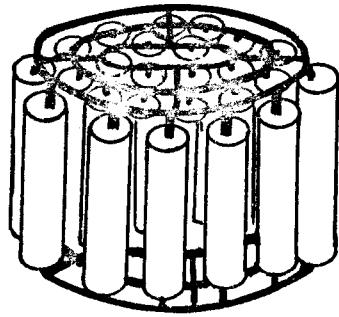


### 3.4 Current and Voltage Probes

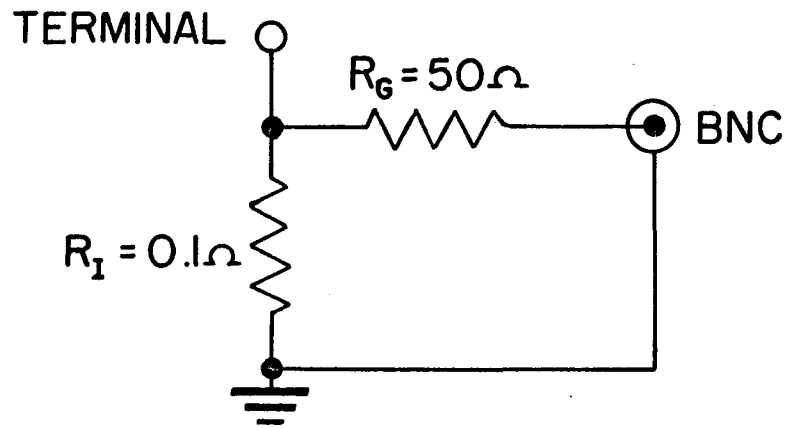
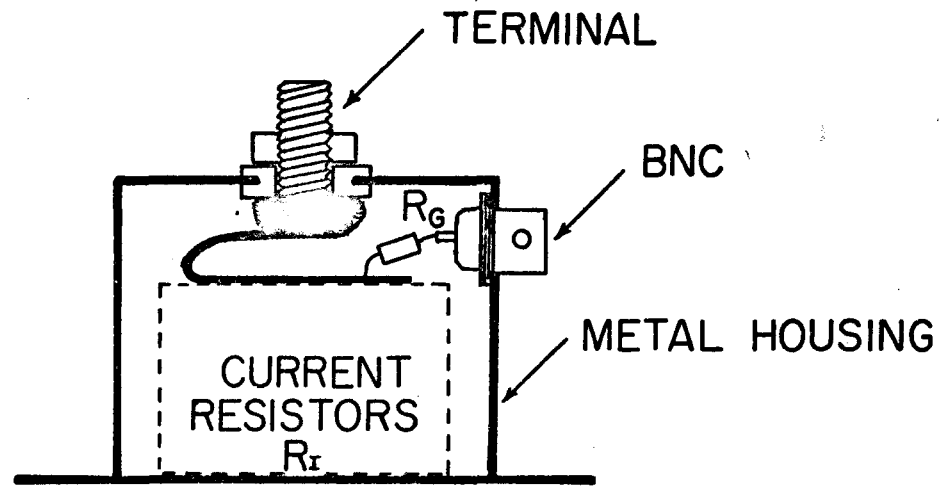
The electrical characteristics of the discharge are important properties of TEA lasers. These are measured using current and voltage probes. The problem with this type of measurement is that the probes and the oscilloscope pick up radiofrequency noise from the discharge. Unless great care is taken, the noise can completely mask any signal that is present. This problem was overcome by careful matching of the probes to the oscilloscope, shielding of the input terminals of the oscilloscope with aluminium foil, and modification of the circuitry of the oscilloscope to reduce internal pick-up. Two types of voltage probes were used; a commercial Tektronix probe (P6015) and a simple high frequency probe (22). Both probes gave the same signal when connected across the laser gain tube. Two types of current probes were also used. One was a current transformer (Pearson Model 411) which was placed around the cathode-to-earth lead, and the other was a simple  $0.1 \Omega$  resistor placed in series with the cathode (22). Once again, both probes gave identical signals, and both were used in the experiments. Figures (3-10) and (3-11) show the current and voltage probes which were designed for use with the TEA laser. More details concerning them, and the electrical properties of the discharge, can be found elsewhere (22). Typical current and voltage pulses are shown in Figure (3-12).

Figure (3-10)

Diagram of the current probe designed for this work



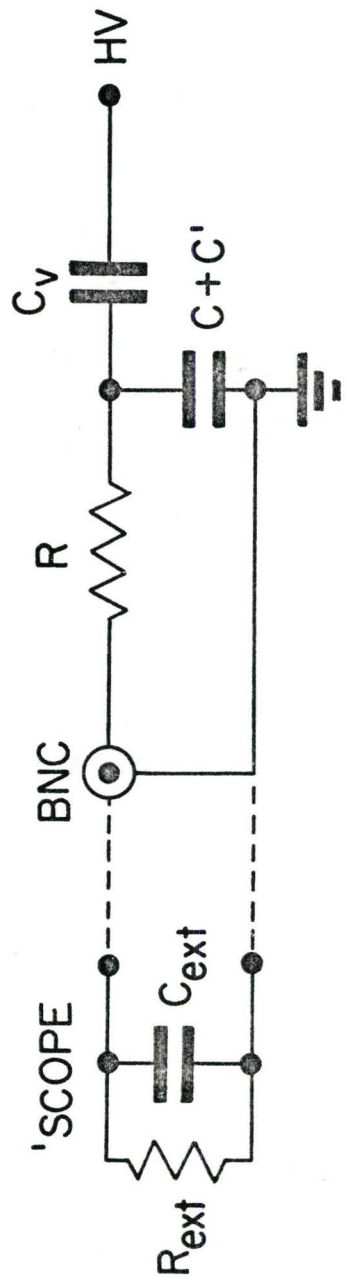
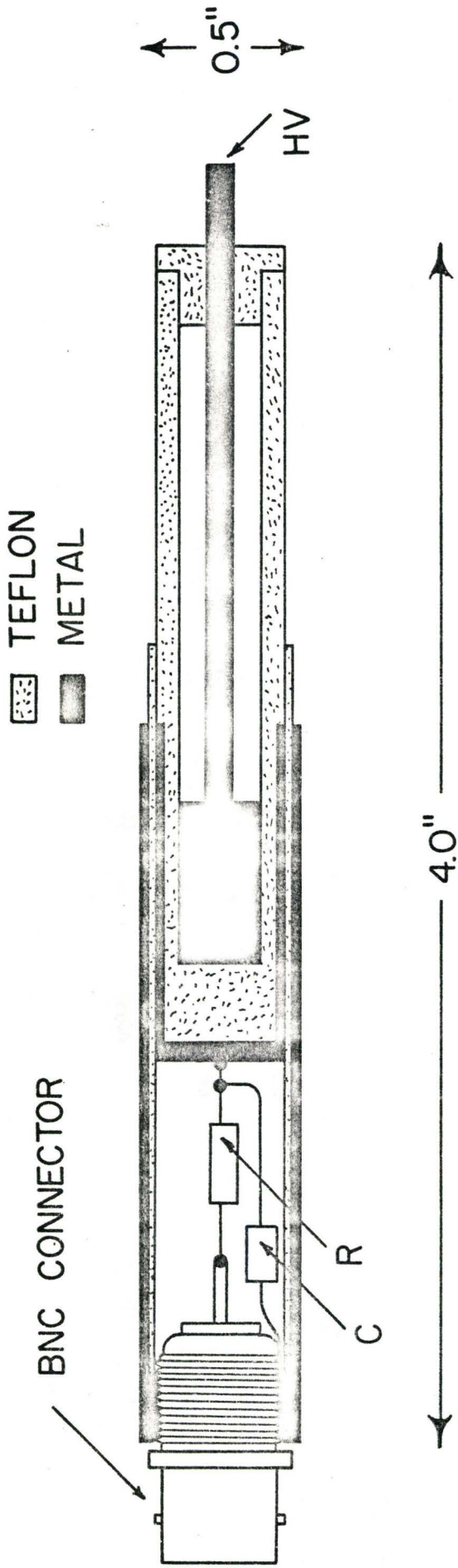
$R_I$



CURRENT PROBE

Figure (3-11)

Diagram of the voltage probe designed for this work



HIGH VOLTAGE PROBE

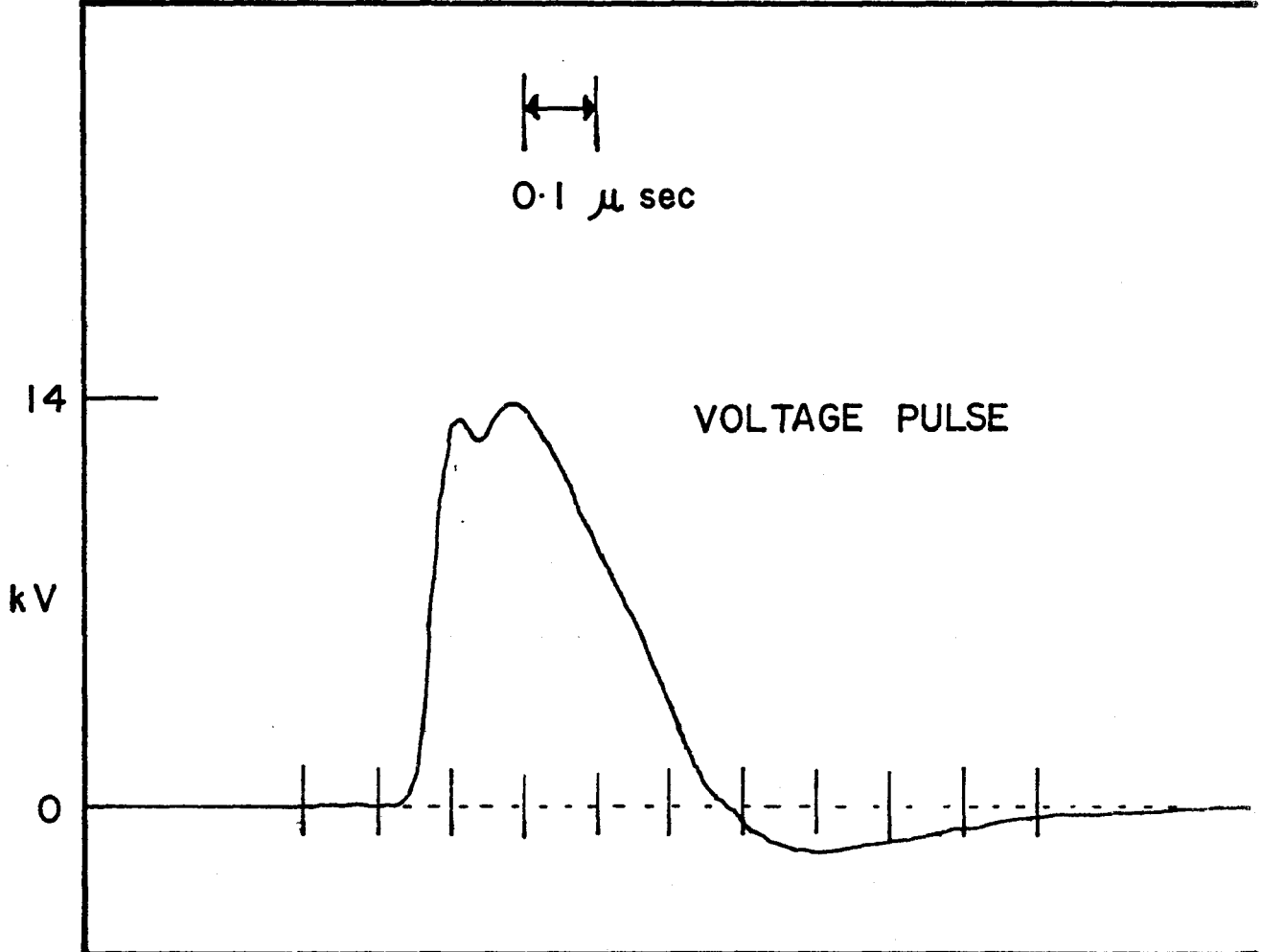
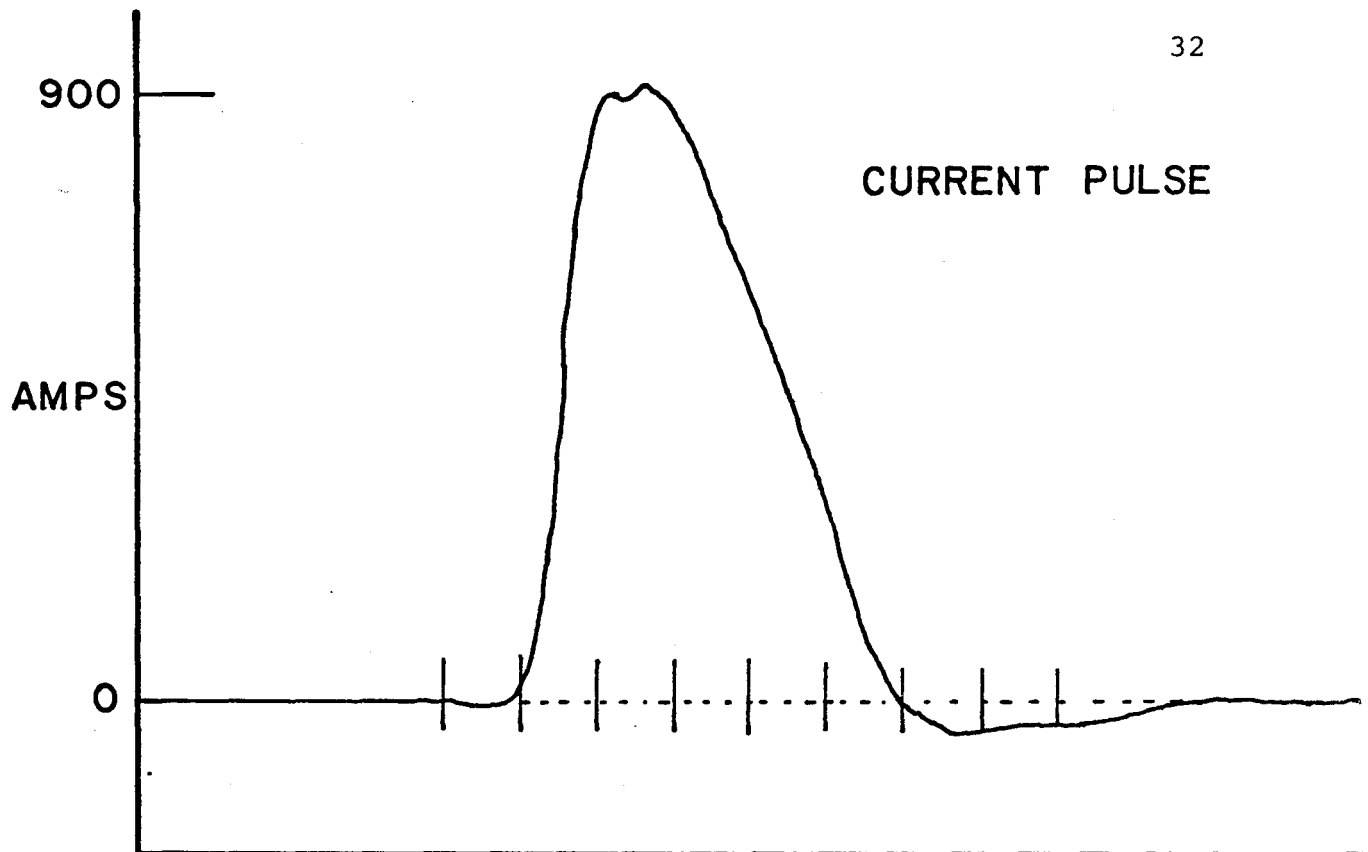
Figure (3-12)

Typical current and voltage pulses

The conditions are a 0.005  $\mu$ F capacitor charged to  
30 kV discharging through a gas mixture of

He 97.2% : CO<sub>2</sub> 2.8%.





### 3.5 Alignment Procedure

Before the system will lase, it must be carefully aligned. The two mirrors must be parallel, and all the NaCl discs in the cavity must have parallel surfaces and be inclined at Brewster's angle. Finally, the region of maximum gain is relatively narrow and is centered on the center of the laser gain tube (6,14). This tube must be positioned on the laser resonator axis. An auxilliary He-Ne alignment laser (Metrologic 410) is used to define the resonator axis between the centers of the two mirrors. (The 10 M mirror is replaced by a blank disc with a small central hole.) All the NaCl discs and the plane mirror are adjusted using the He-Ne beam. The laser gain tube is then centered on the beam, and finally the 10 M mirror is replaced and aligned on back face. The detector is placed in position and the laser gain tube fired. The final alignment adjustments are made by maximising the laser output. This procedure was found to work every time, and the maximum output under standard conditions remained constant from day to day.

When the NaCl discs in the variable loss were rotated, it was found that the laser cavity needed re-alignment. This was due to small wedge angles in the NaCl discs, but posed no great difficulty to correct. All measurements were taken with the laser cavity carefully tuned for maximum output intensity.

### 3.6 Measurements of Pulse Delays

To verify the theory developed in Chapter 2, the time delay,  $t_d$ , between the peak of the current pulse and the appearance of the (steeply) rising edge of the laser pulse must be measured. Both inputs to the oscilloscope are used; one is connected to the current probe, and the other to the detector. The oscilloscope is used in the "Add" mode, and displays a narrow current pulse followed by a wider laser pulse (see Figure (3-13)). It was found that "jitter" of the trace was reduced to a minimum if the oscilloscope was triggered internally on the leading edge of the current pulse.

The method employed to determine the onset of lasing was chosen so that the conditions required to validate the theory given in Chapter 2 are satisfied. This requires that the laser intensity has built up to a value insufficient to significantly saturate the gain. Accordingly, the high-sensitivity gold-doped germanium detector is employed to determine the time at which a predetermined value of the intensity is attained. This intensity is chosen to be small compared to the peak value of the lowest intensity laser pulses on which measurements are made. In all the experimental data taken, the onset of lasing is defined as the point at which the lasing output reaches 0.05 v on the oscilloscope. (The lowest intensity pulses have a peak  $\sim$  0.5 v.)

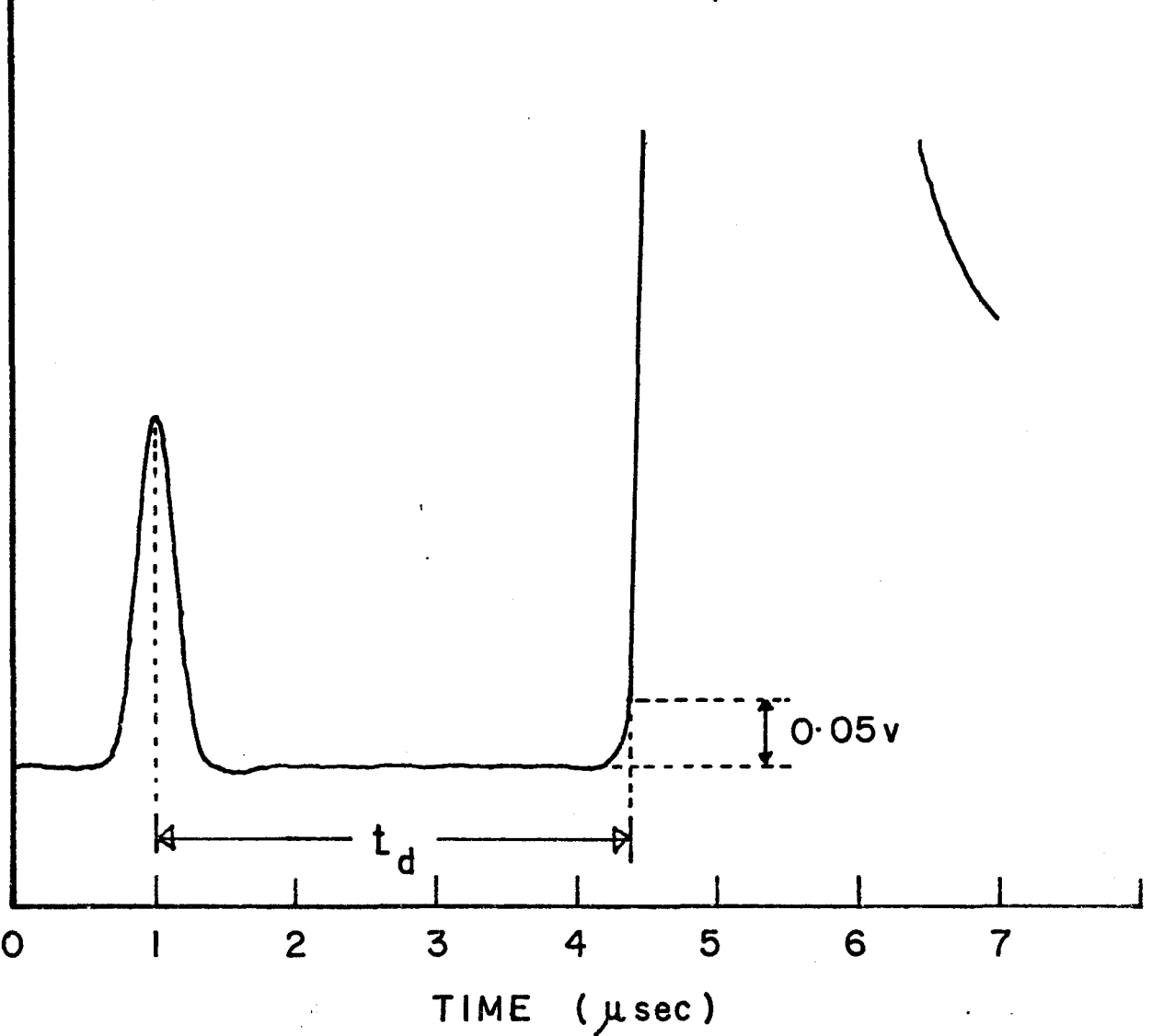
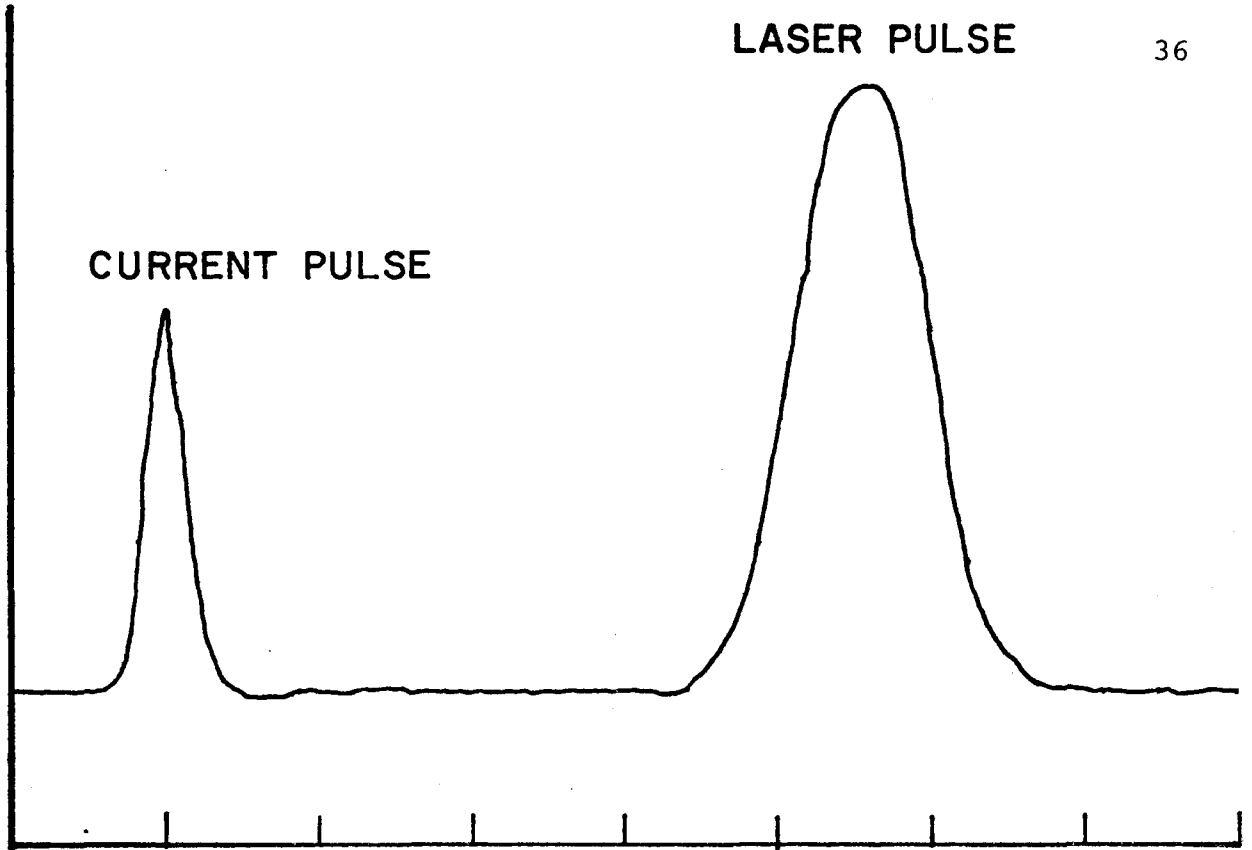
In fact, extreme care in the determination of an operational definition for the onset of significant laser output is not required. This is true because the laser pulse risetime (10% - 90%) is generally short compared to the observed time delays, and the theory is relatively insensitive to the chosen value of the final radiation density employed in equation (2-9). Figure (3-13) is taken from a typical oscilloscope trace, and the value of  $t_d$  is indicated.

The time delay  $t_d$  is measured as a function of voltage for various values of capacitor, cavity loss, and gas mix. The results, and their comparison with theory, are described in Chapter 4.

Figure (3-13)

Typical oscilloscope traces from which  $t_d$  is measured

CURRENT PULSE



CHAPTER IV  
EXPERIMENTAL RESULTS AND DISCUSSION

4.1 Current Pulses

Detailed measurements were made of the current pulses passing through the laser gain tube, and their variation with charging voltage and capacitor. Several gas mixtures were used, but the most detailed work was done on a mixture of He 97.2% : CO<sub>2</sub> 2.8%. The current pulse measurements are important for two reasons. As mentioned in Chapter 2, the simple gain model does not hold for excessively long current pulses, and experimental conditions resulting in long current pulses must be excluded. Furthermore, it is assumed that the gain constant,  $g_0$ , in equation (2-6) is proportional to the integrated current.

From equation (2-9) it can be seen that the time delay,  $t_d$ , is dependent upon the laser gain and the loss for a given laser cavity. Experimentally, the most convenient parameter to vary is the charging voltage applied to a given capacitor, which in turn changes the peak value of the time-dependent gain. It is indicated in Chapter 2 that the peak gain, under appropriate circumstances, is expected to be proportional to the time-integral of the discharge current. It is possible, but inconvenient, to always measure the time-integral of the total discharge current. It is experimentally



much more convenient to employ the capacitor charging voltage as a parameter. Accordingly, measurements were made of the integrated current as a function of the charging voltage for several capacitor values employed in subsequent measurements. The time-integration of the current was obtained by photographing the oscilloscope display of the current pulse and applying a gravimetric technique to obtain the integral of the current pulse. Figure (4-1) shows the variation of the integrated current so obtained as a function of the charging voltage for a  $0.01\mu\text{F}$  capacitor. The result is typical of that obtained for other capacitor values. Data taken for  $0.01\mu\text{F}$  and  $0.005\mu\text{F}$  capacitors is given in Appendix II. Observe from Figure (4-1) that the integrated current and the charging voltage are linearly related over most of the range of voltage values. This linear relationship begins to fail as the value of the charging voltage approaches the discharge breakdown voltage. This region also corresponds to the situation in which the widths of the current pulses become large. As a consequence, since data obtained with long current pulses are rejected, the integrated current and the charging voltage are linearly related in the experimental region of interest. Thus, provided that the time-integral of the current is directly proportional to the gain, it has been shown that the gain is proportional to the charging voltage on the capacitor. In addition, it is found that the integrated current at a given charging voltage is proportional to the value of the

discharge capacitor. It follows that, with the proviso stated above, the gain varies directly as the capacitor value for a given charging voltage. Consequently, the gain can be varied over a wide range in a known way by varying the charging voltage and the discharge capacitor. The existence of a linear relationship between the gain of a TEA CO<sub>2</sub> laser amplifier tube and the charging voltage has been observed by Robinson <sup>(11)</sup>, employing direct gain measurement techniques. He also reports that the measured gains at a given voltage changed directly as the capacitor value used. This is in agreement with the observations described above and lends considerable confidence to the use of the charging voltage as a suitable parameter for the laser tube low signal gain. This parametrisation of the gain finds additional justification from a number of experimental observations, of a generally self-consistent nature. For example, the same laser output is obtained if the discharge capacitor value is reduced and the charging voltage is proportionately increased. In each case, the same loss must be inserted into the cavity to just prevent lasing. Furthermore, the superposition of the laser pulse time delay curves as the capacitor value is changed is excellent when the appropriate scaling factor is applied to the charging voltage. The data is generally presented in terms of a normalised charging voltage, which corresponds to the actual discharge voltage applied to a given capacitor, scaled by the ratio of the capacitor value to that

of the largest capacitor value employed ( $0.01\mu\text{F}$ ).

It was indicated previously that, for reasons of experimental and theoretical convenience, experimental data obtained with excessive current pulse lengths were rejected. In order to do so, it is necessary to know the variation in the current pulse lengths as the capacitor value and the charging voltage are varied. Figure (4-2) shows the variation of the pulse width as a function of charging voltage for several capacitor values. Observe that, as the charging voltage is reduced toward the breakdown voltage of the gain tube ( $\sim 12\text{kV}$ ), the current pulses become longer. In addition, the width of the current pulse increases, for a given charging voltage, as the value of the capacitor increases. The rise-time of the pulse remains almost constant, it is an increase in the fall-time which causes the increased width. The data shown in this figure were taken with a gas mixture corresponding to the one on which most of the detailed time-delay data were obtained. On the basis of this data no results employing the  $0.02\mu\text{F}$  capacitor were used and in general, only observations obtained for charging voltages above  $20\text{kV}$  were utilised, except for the smallest capacitor. More data concerning the current pulse width can be found in Appendix II. Note that the effect of increasing current pulse width on the measurement of laser pulse time delays is mitigated somewhat by the fact that these delays increase as the charging voltage (and hence the gain) decreases. Further details of current and

voltage pulses in TEA CO<sub>2</sub> lasers can be found in references [22] [23].

Figure (4-1)

The variation of the time-integrated current pulse with  
the capacitor charging voltage  $V_C$

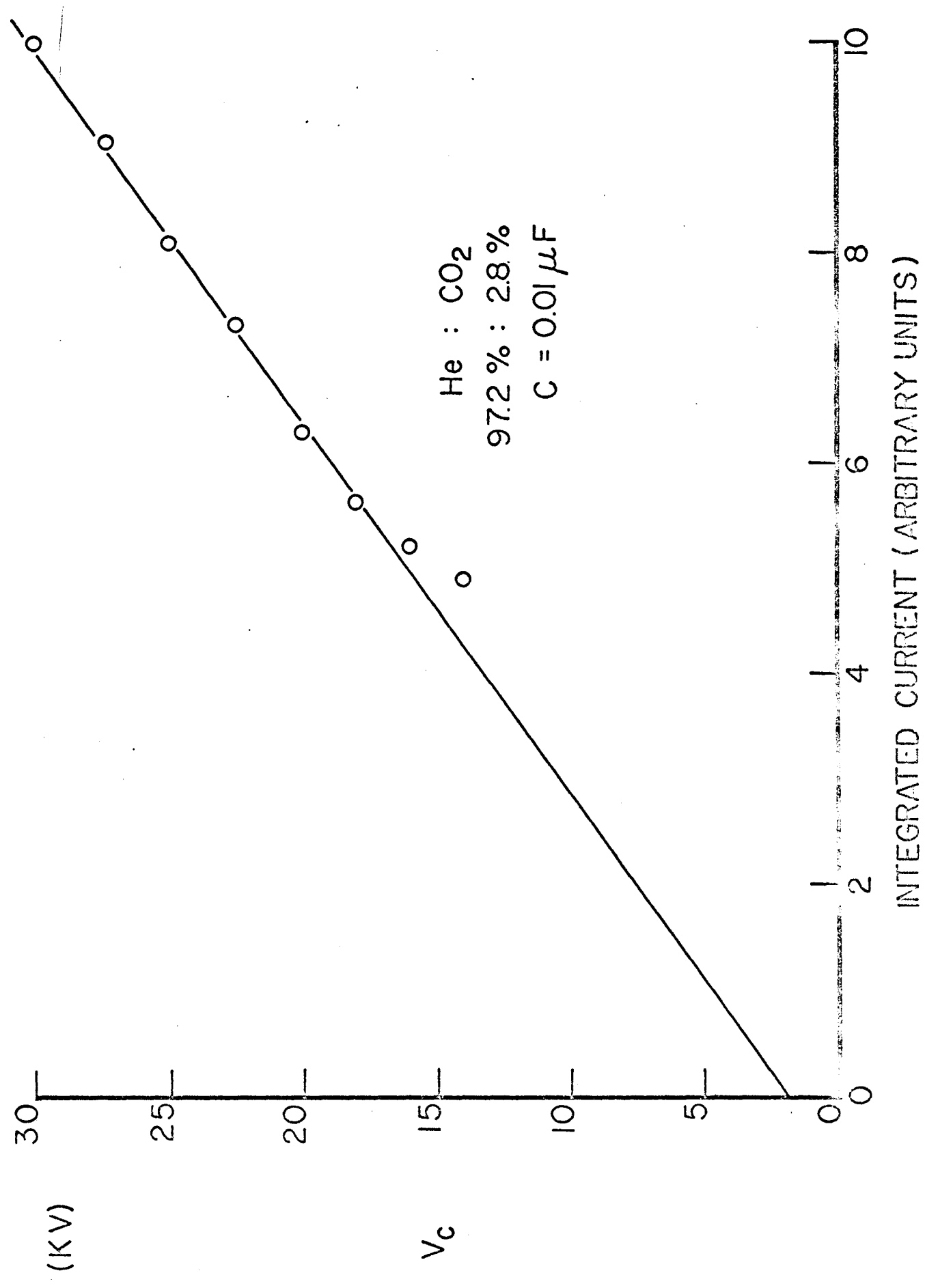
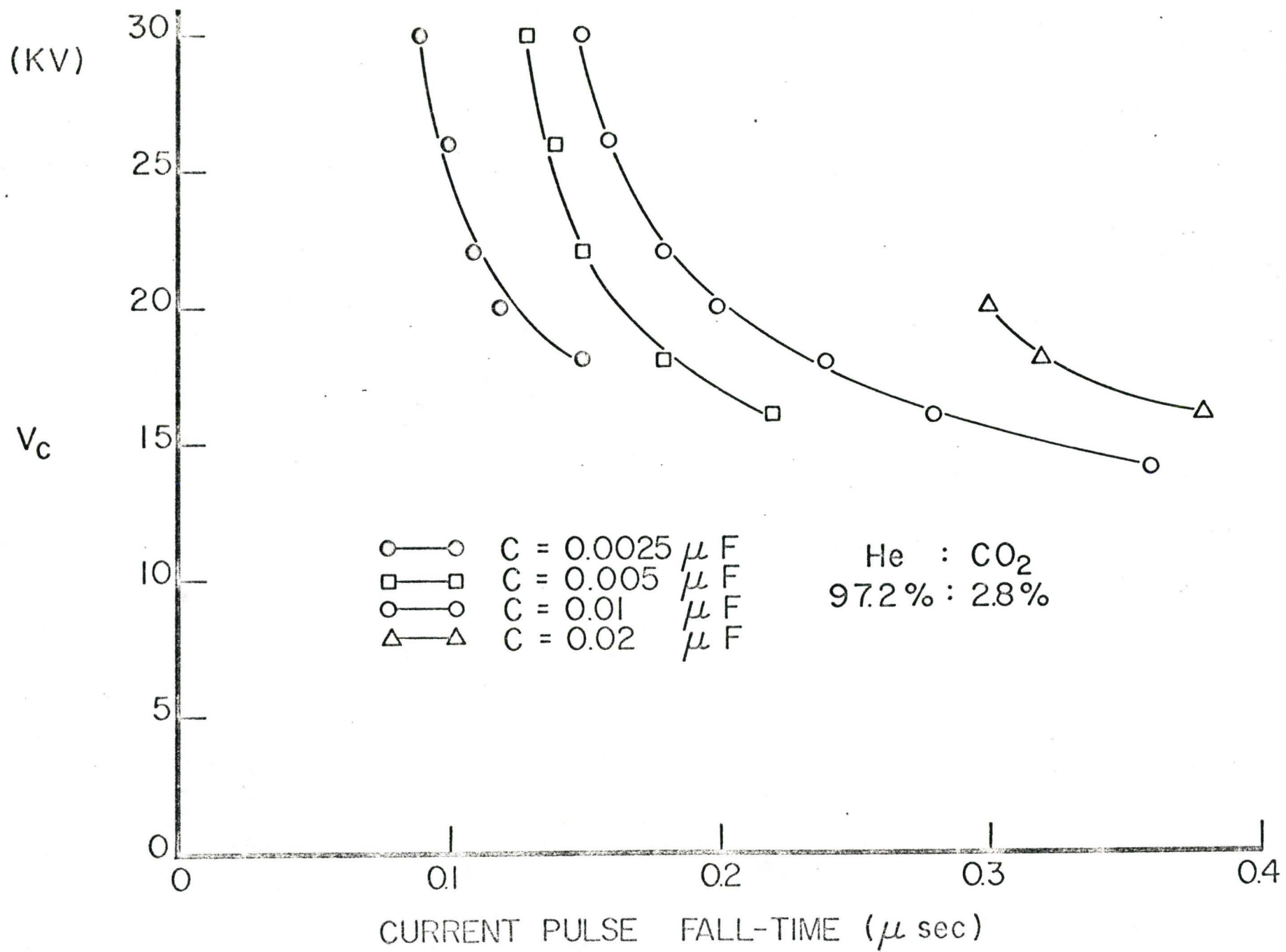


Figure (4-2)

Plots of the current pulse fall-times (peak to half-height) against the capacitor charging voltage  $V_c$  for several capacitor values





## 4.2 Laser Pulse Delays

Experimental curves are obtained for the variation of the time delay,  $t_d$ , with normalised voltage. Three different capacitors are used ( $0.01\mu\text{F}$ ,  $0.005\mu\text{F}$  and  $0.0025\mu\text{F}$ ), and several different gas mixes. The next step is to attempt to fit the theory given in Chapter 2 to the experimental curves obtained. This was done using a CDC 6400 computer to obtain theoretical time delay values from equations (2-9) and (2-10). The program used gave the time delay as a function of normalised voltage (gain is proportional to voltage), and also had provision for the variation of the values of the peak gain (i.e. gain when normalised voltage equals 30kV), cavity loss,  $T_1$  and  $T_2$ , and  $\ln(\rho_f/\rho_i)$ . Approximate values were used initially for all these factors. The approximate values were a blend of common sense and available literature data. These factors were then varied in a sensible manner until the best fit with the experimental data was found. Further details of the fitting procedure are given in the next section.

Figure (4-3) shows the variation in the time delay,  $t_d$ , as a function of the normalised charging voltage. The continuous line represents a theoretical fit to the data. Each of the experimental points represents an average over several individual points and is accurate to within 5-10%. The high value occurs only for points with a large time delay, where the system is extremely sensitive to small

variations in the gain or loss. The gas mixture used to obtain the data in Figure (4-3) was 97.2% He and 2.8% CO<sub>2</sub>. Figure (4-4) is a similar set of data for a gas mixture of 94.4% He and 5.6% CO<sub>2</sub>. Once again the continuous line represents a theoretical fit. Similar investigations have been carried out for other gas mixtures, including nitrogen; the data is given in Appendix II and the results obtained will be discussed in a subsequent section.

Since the fitting of the theory to experiment involves the variation of a number of parameters it is important to pin down the various parameters as much as possible by varying another parameter in addition to the gain. This can be done by changing the laser cavity loss by known amounts using the variable loss. Figure (4-5) displays the resulting family of curves typically obtained in this way. The continuous curves represent a theoretical fit to the data. In this fit, only the loss is changed, and all other parameters are fixed. It can be seen that a good fit to the data is obtained.

Figure (4-3)

The time delay ( $t_d$ ) of the onset of lasing with respect to the peak of the current pulse as a function of normalised voltage

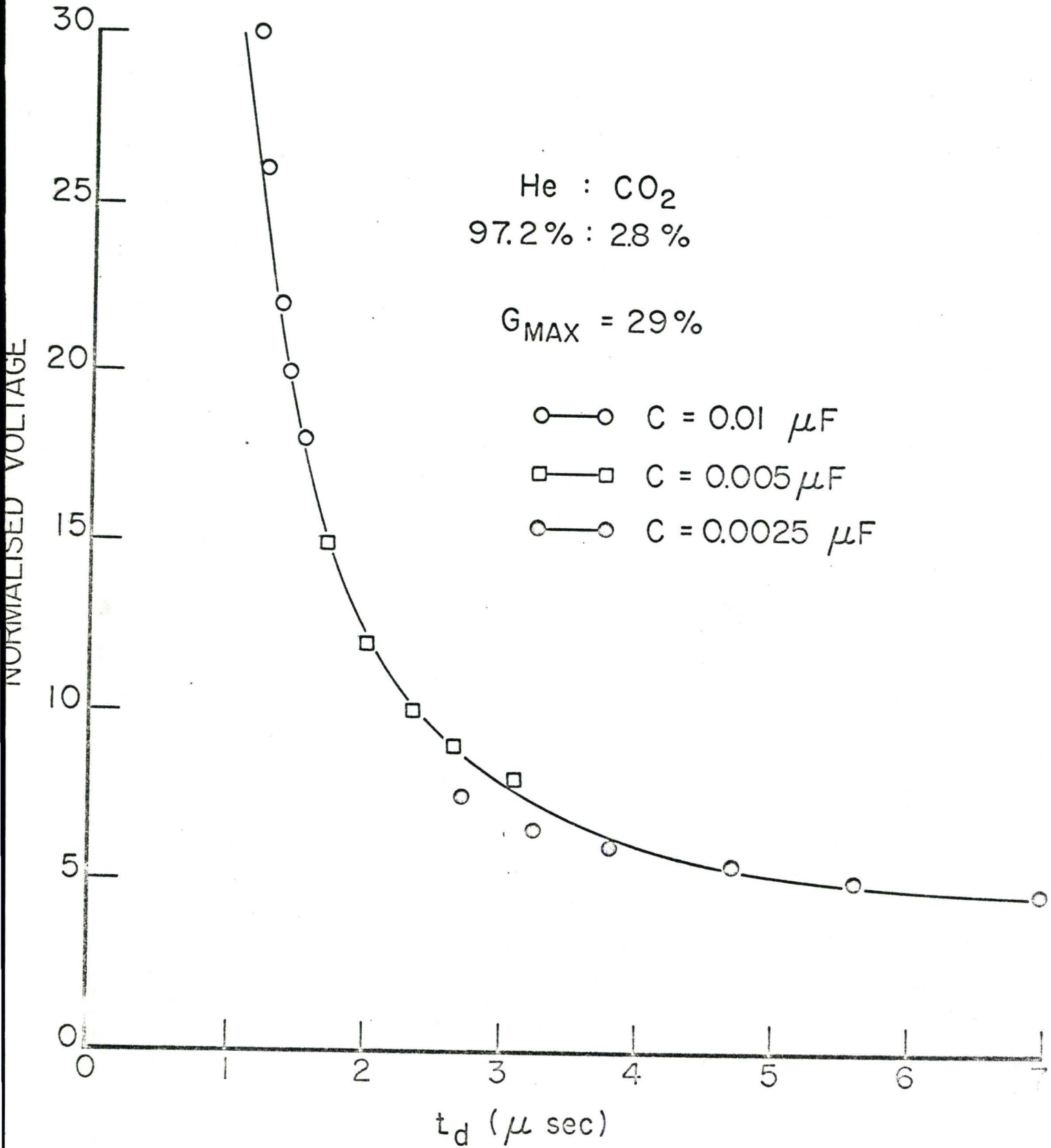


Figure (4-4)

The time delay ( $t_d$ ) as a function of normalised voltage for  
a different gas mixture

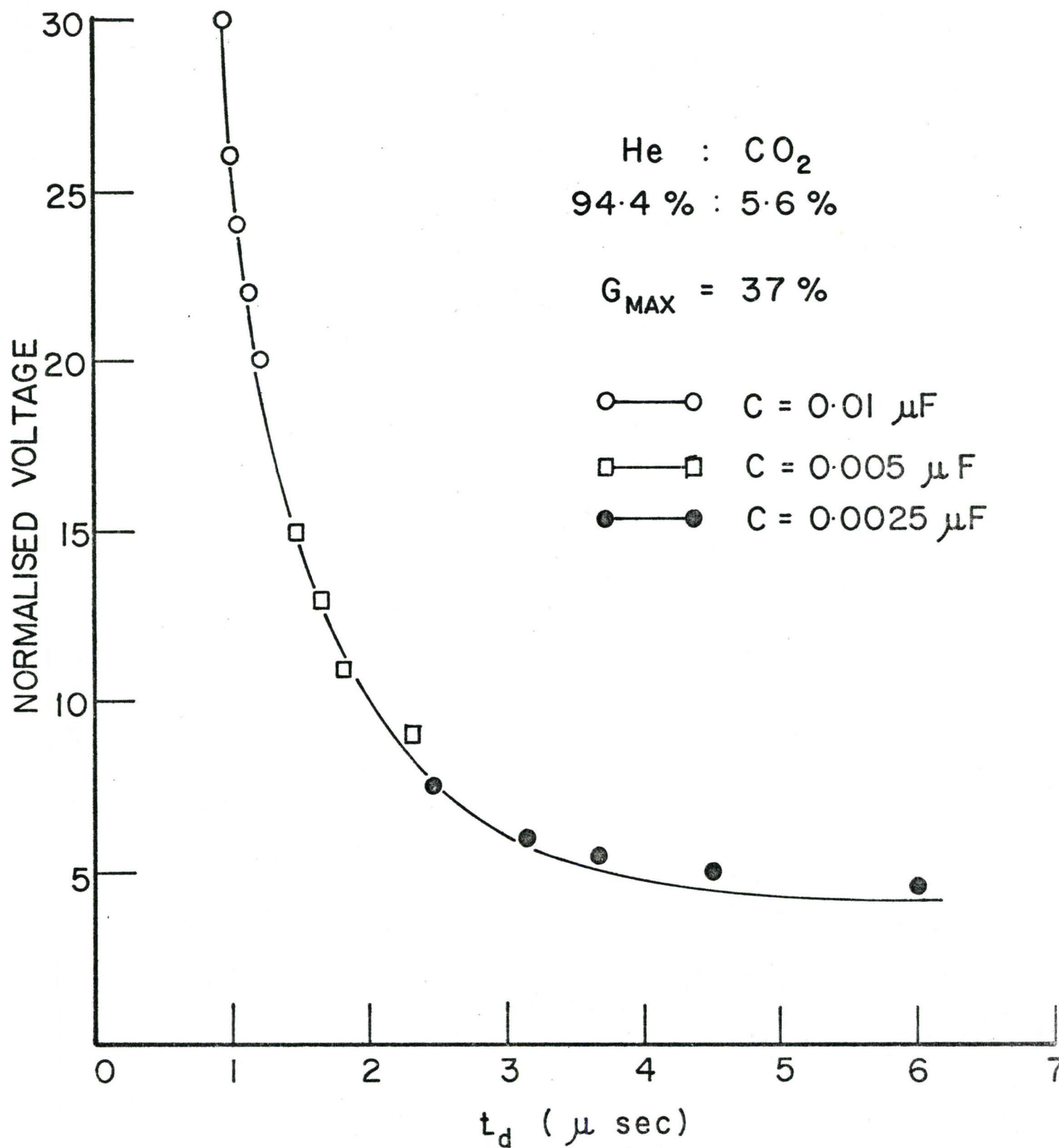
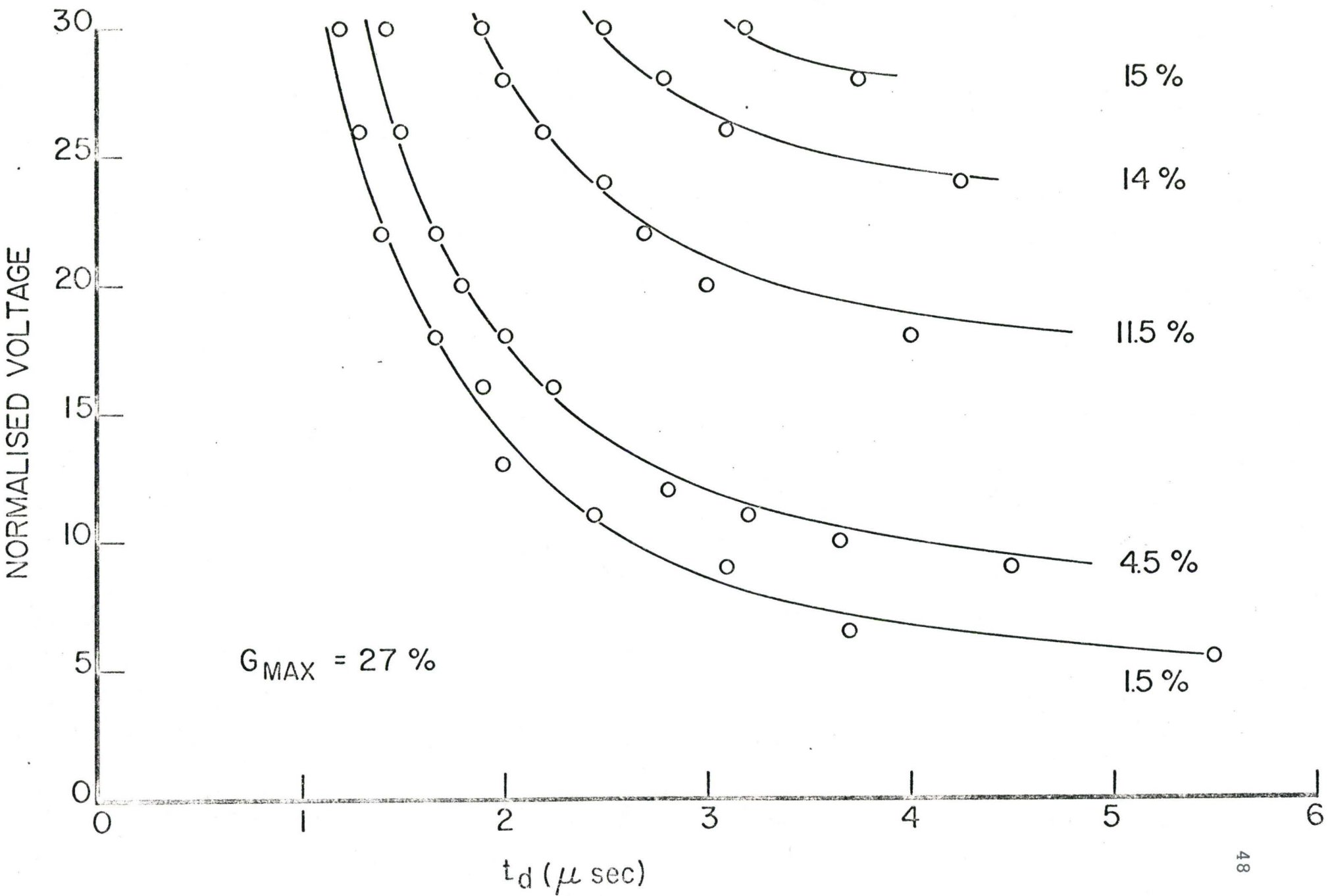


Figure (4-5)

Plots of the time delay of the onset of lasing with respect to the current pulse peak, against normalised voltage for several values of the cavity loss



CAVITY LOSS



### 4.3 Contact between Theory and Experiment

The measurement of the gain obtained by fitting the theoretical expression for  $t_d$  to the experimental data can be seen from equation (2-9) to be dependent upon the value of  $\ln(\rho_f/\rho_i)$ . It is possible to make theoretical estimates of this parameter; however the use of calculated values for the factor  $\ln(\rho_f/\rho_i)$  has been avoided by employing the following (calibration) strategy. For any particular experimental situation, the shape of the laser pulse delay against gain (in arbitrary units) can be fitted to the functional form of the time-dependent gain with an unassigned value of the peak gain. This allows the determination of  $T_1$  and  $T_2$ . Now, the loss which must be inserted in the laser cavity to just prevent the onset of lasing is measured. This, together with a knowledge of the time-dependence of the gain, permits a direct estimate of the gain peak, independent of  $\ln \frac{\rho_f}{\rho_i}$ . This procedure, together with the known values of the time delay of the onset of lasing, can be used to determine experimentally the appropriate value for  $\ln \frac{\rho_f}{\rho_i}$ . The method can be refined in a self-consistent fashion using different values for the charging voltage. The value of  $\ln(\rho_f/\rho_i)$  so obtained lies within the directly estimated limits which can be placed on this parameter.  $\rho_f$  can be estimated from the detector characteristics and the transmission of the output mirror.  $\rho_i$  is more difficult to estimate, but can be found approximately by considering the spontaneous emission from the excited

$\text{CO}_2$  molecules during the early part of the time-delay  $t_d$ . Such a direct estimate of  $\rho_f/\rho_i$  is probably only accurate to a factor 100 (or 15% in  $\ln(\rho_f/\rho_i)$ ), but the theory is relatively insensitive to the chosen value of  $\ln(\rho_f/\rho_i)$ . This is true because the laser pulse risetime (10 - 90%) is generally short compared with the observed time delay. Throughout this work, the measured gain peaks for the various gas mixtures are determined solely by the inserted loss measurements, and not by any arbitrary theoretical value of  $(\rho_f/\rho_i)$ . Once the value of  $\ln(\rho_f/\rho_i)$  has been obtained, the fitting of experiment and theory is relatively straightforward. Reasonably accurate fits can be obtained by comparing data such as that illustrated in Figures (4-3) and (4-4) with an appropriate range of computer-generated curves. Refinements of the fit are made using the observations that the short delay data is essentially determined by the peak gain and  $T_1$ , whereas the long pulse delays are sensitive to the peak gain,  $T_2$  and the cavity loss. The fit can be further refined by fitting to a family of curves such as those shown in Figure (4-5).

#### 4.4 Results and Discussion

The most detailed fit was made to a particular  $\text{CO}_2$ :He gas mixture of approximate proportion 2.8% : 97.2%. The fitting procedure gave the following values for the gain and loss parameters. For a capacitor value of  $0.01\mu\text{F}$  and a charging voltage of 30kV, the peak gain was found to be 29% for a new tube and 27% for the same tube after several hours of operation. The value of  $T_1$  was 1  $\mu\text{sec}$  and of  $T_2$  was 8  $\mu\text{sec}$ . The peak of the gain occurs approximately 2.3  $\mu\text{sec}$ . after the current pulse. When appropriate adjustment for different operating conditions is made to the data reported by Robinson (11) for the peak value of the gain/pass and the time at which the peak occurs, the agreement between the two sets of data is better than 10% in both cases. Less detailed fits have been made for other  $\text{CO}_2$ :He gas mixtures. In particular, for a 5.6% : 94.4% mixture the peak gain is found to be 37% (again in good agreement with Robinson); all other parameters remain the same. Similar results were obtained for a 1.4% : 98.6% mixture; the peak gain was found to be close to 13%.

In addition to the results obtained with nitrogen-free gas mixtures, some preliminary analysis has been made of a gas mixture containing nitrogen. The parameter fit for a  $\text{CO}_2$ : $\text{N}_2$ :He mixture of 3% : 3% : 94% gave the following results:  $T_1 = 2 \mu\text{sec}$ .,  $T_2 = 20 \mu\text{sec}$ . and the peak gain/pass was 47%. This combination of  $T_1$  and  $T_2$  leads to a value of 5.1  $\mu\text{sec}$ . for the time after the current pulse at which the gain reaches



its peak value. These values are also in excellent agreement with the data given by Robinson.

The fit between theory and experiment gives values for the average cavity loss per pass in the absence of additional inserted loss, as well as the parameters describing the time-dependent gain. For the experimental set-up employed in these experiments, the cavity loss values so obtained are typically close to 1.5%. This value is very reasonable, since the average loss per pass due to mirror losses lies between 1 and 1.5%. The losses at the Brewster's angle NaCl windows are very small, since the insertion of the variable loss makes only a small change in laser output; whereas using this unit to insert an additional loss of 1% into the laser cavity causes very large changes in the laser pulse intensity.

The precision of the fitting process is not the same for all the parameters. A precise estimate of the errors for each parameter is a little difficult to obtain. However, the value of the peak gain is determined mainly by the precision of the inserted loss and to a lesser degree by the values of  $T_1$  and  $T_2$ . The gain values obtained are probably accurate to within 10%, provided that the inserted loss values are accurate to the same degree. The value of  $T_1$  is estimated to be good to approximately 20%, obtained by comparing observations with computer-generated curves having parameter variations in this range. A similar technique applied to  $T_2$  shows that its value almost certainly lies between 6  $\mu\text{sec.}$  and 12  $\mu\text{sec.}$  for

the He 97.2% and CO<sub>2</sub> 2.8% gas mixture. In general the computer fit is relatively insensitive to the value of T<sub>2</sub>. Chapter 5 describes a technique which is used to determine the values of T<sub>2</sub> more accurately. The values obtained for the parameters describing the time-dependent gain are in good agreement with Robinson's data concerning the time to reach the peak gain after the discharge current pulse. However, the accuracy claimed for his data is fairly low, and separate data concerning T<sub>1</sub> and T<sub>2</sub> is not given. Extrapolation of data (24,25) concerning the lifetimes of the laser levels to atmospheric pressure gives values of T<sub>1</sub> and T<sub>2</sub> relatively close to those reported here, particularly when the uncertainties associated with unknown discharge conditions are taken into account. Recently, the observation of a time-dependent lens effect in helical TEA CO<sub>2</sub> lasers has been reported (6,26). It is expected that such effects will be of negligible importance for the measurements reported here. This is because these lens effects are thermal in origin and were observed at rather high dissipation levels in the discharge. In the present experiments, such effects might be important for the longer delays between the current pulse and the onset of lasing. However, such delays only occur for very small energy dissipation levels in the discharge, where thermal effects are minimal.

The values of peak gain obtained by the technique described here correspond to a wavelength average over the gain

line, near line centre, for the rotational level which has maximum gain. This technique is such that it naturally selects the line with the highest gain, and those modes within the line which experience the highest gain.

## CHAPTER V

### A MORE ACCURATE MEASUREMENT OF $T_2$ USING AN ADDITIONAL GAIN TUBE

The technique described so far is a useful method for determining the peak gain and the cavity loss. However, it is less sensitive to the exact time-dependence of the gain, in particular the decay-time  $T_2$ . The technique described in this Chapter provides a simple and accurate method of measuring  $T_2$ . An additional short gain tube is introduced into a laser cavity already containing a laser gain tube. The two tubes are discharged separately but are arranged so that they can be fired with a controllable time delay between the discharge current pulses. The time delay of the onset of lasing with respect to the laser tube current pulse is changed by firing the additional tube in the laser cavity. Observed time delay changes can be related to the simple theory given in Chapter 2 and further explained in the next section. The fit between theory and experiment allows the determination of parameters describing the time-dependent gain. This two-amplifier technique has the advantage of improved sensitivity; in addition, it allows more direct probing of the decay-time of the amplifier gain.



### 5.1 Theory

Equations (2-8) and (2-9) of Chapter 2 are reproduced for convenience.

$$\ln(\rho_f/\rho_i) = \int_{t_{th}}^{t_f} [g(t) - 1/\tau_c] dt \quad (2-8)$$

$$\begin{aligned} \ln(\rho_f/\rho_i) = & g'_0 \exp(-t_{th}/T_2) [T_2(1-\exp(-t_f/T_2)) - t_f] \\ & - g'_0 \exp(-t_{th}/T_1) [T_1(1-\exp(-t_f/T_1)) - t_f] \end{aligned} \quad (2-9)$$

These expressions determine the time delay, with respect to the discharge current, of the build-up of a radiation density  $\rho_f$  from an initial density  $\rho_i$ . Equation (2-8) applies for a one-amplifier system and for radiation densities which do not appreciably saturate the gain. Evidently, an equation similar to equation (2-8) can be written for the two-amplifier case, VIZ:

$$\ln(\rho_f/\rho_i) = \int_{t'_{th}}^{t'_f} (g_1(t) + g_2(t+t_0) - 1/\tau_c) dt \quad (5-1)$$

where  $g_1$  and  $g_2$  are the gains in the two amplifiers, and  $t'_{th}$  is now determined by :

$$g_1(t'_{th}) + g_2(t'_{th} + t_0) = 1/\tau_c \quad (5-2)$$

and  $t_0$  is the time delay introduced between the firing of the two tubes. (Compare with equation (2-10)).

In the experiments to be described in a subsequent section, a comparison is made between the observed time delay when the laser and amplifier tubes are both fired, and the time delay for the laser tube alone. In both cases, the time delays are measured to the same (small) value of the output intensity (0.05 v). Consequently, from equation (2-8) and (5-1), it follows that :

$$\int_{t_{th}}^{t_f} (g_1(t) - 1/\tau_c) dt = \int_{t'_{th}}^{t'_f} (g_1(t) + g_2(t+t_0) - 1/\tau_c) dt \quad (5-3)$$

where  $g_1(t)$  is the gain in the laser tube. This equation may be re-written in the form

$$\begin{aligned} \int_{t'_f}^{t_f} (g_1(t) - 1/\tau_c) dt - \int_{t'_{th}}^{t_{th}} (g_1(t) - 1/\tau_c) dt \\ = \int_{t'_{th}}^{t'_f} g_2(t+t_0) dt \end{aligned} \quad (5-4)$$

In particular, if the second integral on the left of the equation is small compared with the other terms, and  $g_1(t)$  varies little between  $t_f$  and  $t'_f$ , equation (5-4) may be

written as :

$$\int_{t'_{th}}^{t'_{f}} g_2(t+t_0) dt = K(t_f - t'_f) \quad (5-5)$$

where K is a constant.

## 5.2 Experimental Arrangement

The apparatus employed in these experiments is shown in Figure (5-1). The only change from the previous experimental arrangement is the addition of the small gain tube into the laser cavity. This tube has the same helical design, but is 12 inches long and has a pitch of 6 inches. It is fired by an identical circuit to that shown in Figure (3-2), but is completely independent of the main laser tube circuit. The two low-voltage pulse generators are arranged so that the unit controlling the main laser tube is fired by a timing signal from the short-tube pulse-generator. This arrangement permits the introduction of a variable delay between the firing of the two tubes. The discharge currents of the two tubes are monitored using the current probes described in Section 3.4. Both the current pulses and the laser output are displayed on the oscilloscope. In all other respects, the experimental apparatus and procedures are identical to those described in Chapter 3.

Figure (5-1)

Schematic diagram of two-amplifier apparatus

The total cavity length is now 250 cms.

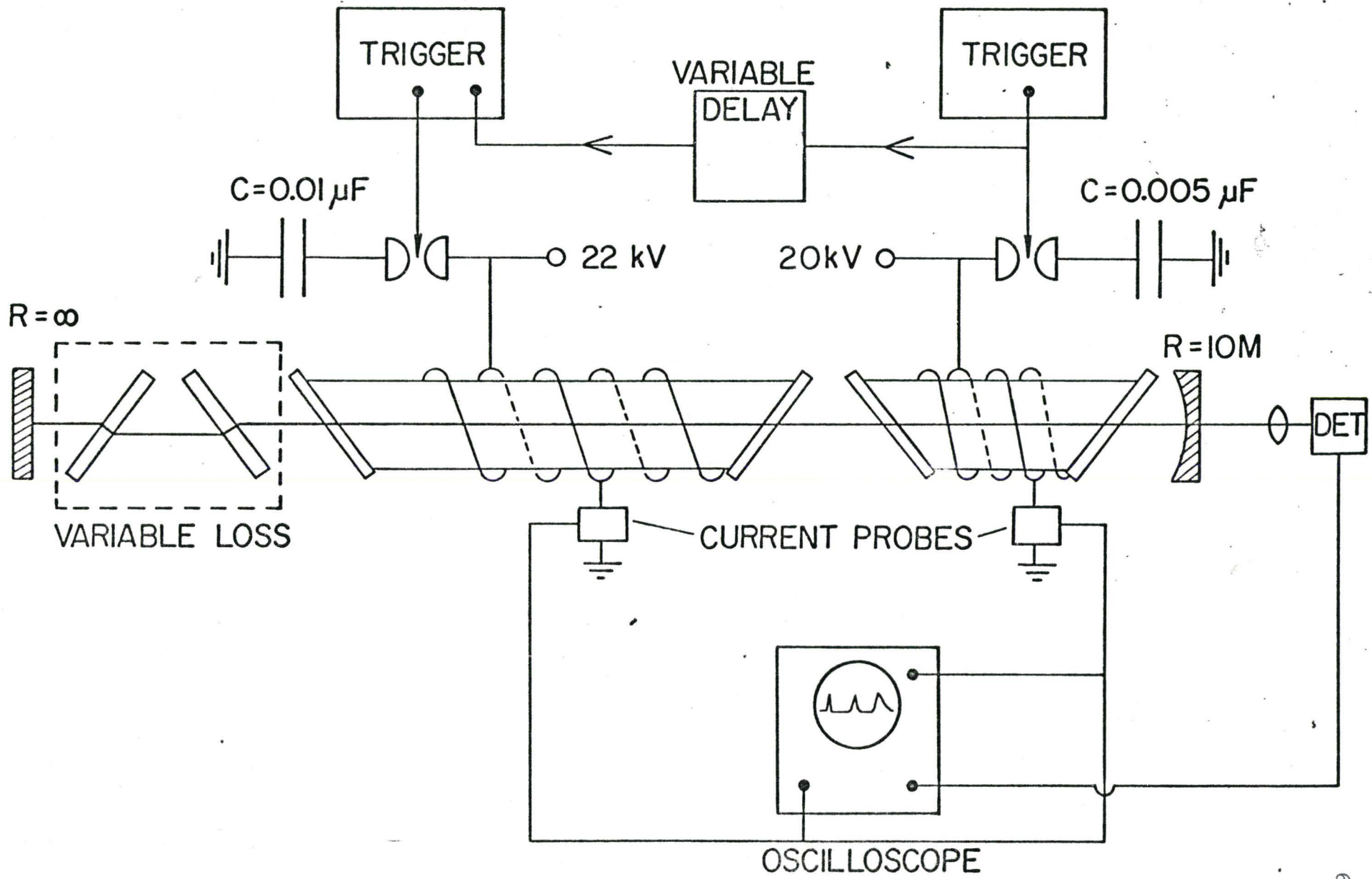
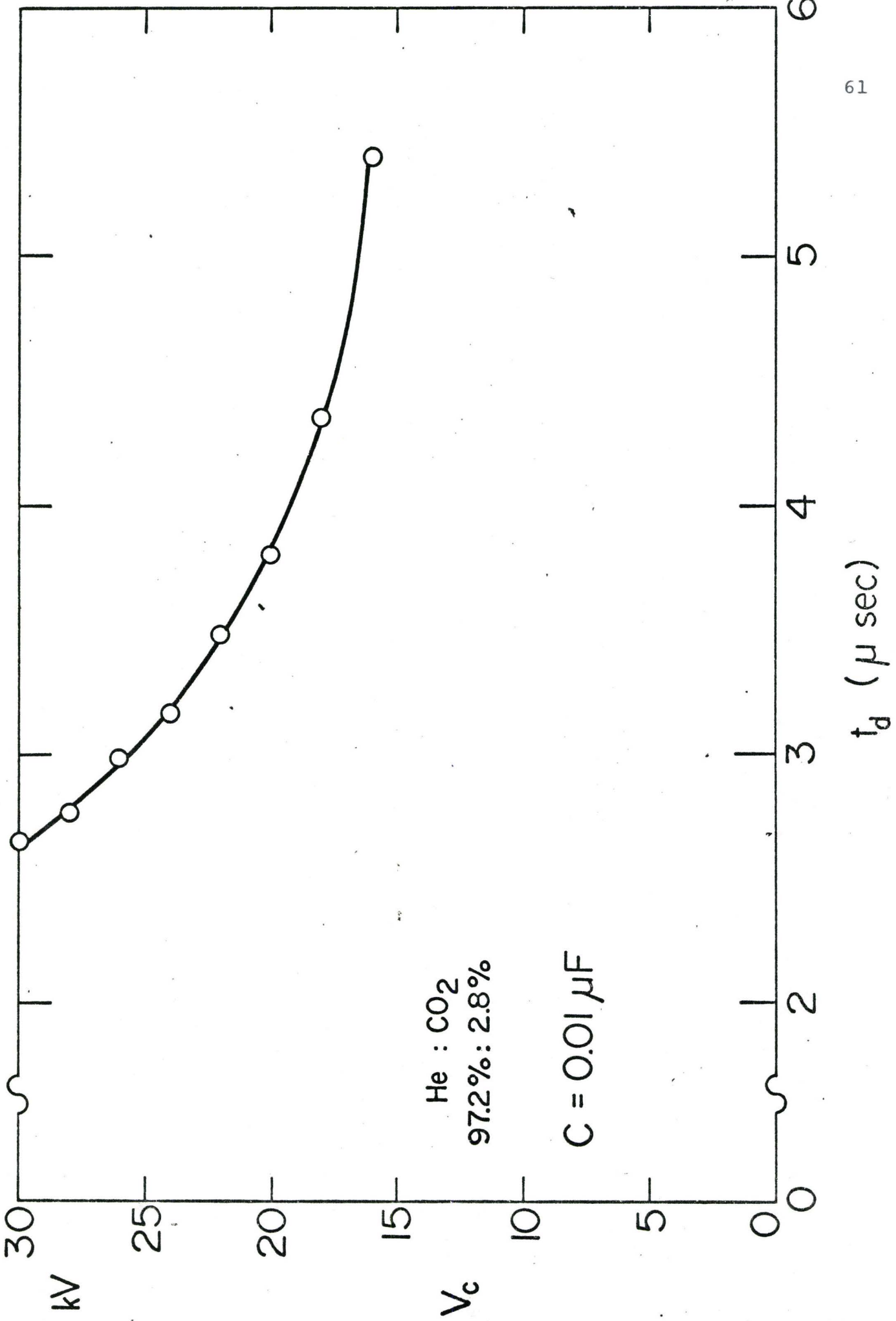


Figure (5-2)

Variation of time delay ( $t_d$ ) with charging voltage  
for a total cavity loss of 8%





### 5.3 Experimental Observations and Discussion

The extra amplifier tube is one-third of the length of the main laser tube. As a consequence the gain per pass through the added tube is considerably less than that of the main amplifier for similar values of the current passing through the individual discharges. This condition is important for the measurements described, since it is necessary to avoid lasing action when the small tube alone is fired. Suppression of lasing action is achieved by the insertion of a cavity loss sufficient to prevent lasing with the small tube alone, but not large enough to suppress lasing with the main amplifier only. In fact, the total cavity loss was greater than the peak gain of the small tube.

The initial step in the experiment is to measure the time delay,  $t_d$ , of the laser output pulse as a function of voltage for the laser amplifier alone. Figure (5-2) shows this variation in  $t_d$  as a function of voltage with a cavity loss of 8%. It is evident that small changes in charging voltage can produce large changes in the time delay of the onset of lasing. As the peak gain of the laser tube is proportional to charging voltage, the sensitivity of  $t_d$  to gain changes is increased as the charging voltage of the main amplifier is reduced. For this reason, the laser gain tube was

operated at 22 kV, corresponding to a  $t_d$  value of  $3.4\mu\text{sec}$ . Longer time delays give a higher sensitivity, but the results are more erratic. The chosen time delay has an additional advantage in that it lies close to, but somewhat greater than, the time at which the gain peaks (see Chapter 4). The gain varies very slowly near the peak for the gas mixtures investigated, and thereby permits a considerable simplification of the procedure for fitting theory and experiment. In order to determine a value for  $T_2$ , the experiment proceeds as follows. The small gain tube is arranged to fire in advance of the main laser tube, and the change in the value of  $t_d$  from that obtained with the main amplifier only is observed. This measurement is repeated for a number of values of the time difference between the firing of the two tubes. Attention has been restricted to relatively large values of the time-advance of the firing of the small amplifier relative to the main amplifier. However, the method can also be applied to obtain values of  $T_1$  by employing amplifier time delays close to the coincidence of firing. (The analysis of this type of data would be more difficult than the analysis to obtain values of  $T_2$ ).

The data obtained by measurements of the type indicated above have been analysed in the following way. For values of  $t_0$  (the time difference between the firing of the two tubes) considerably larger than  $T_1$ , the time-dependence of the gain,  $g_2(t+t_0)$  in the small amplifier tube is simply an exponential

decay. In this case, equation (5-5) can be written :

$$g_{20} \int_{t'_{th}}^{t'_f} \exp[-(t+t_0)/T_2] dt = K(t_f - t'_f) \quad (5-6)$$

which, to a good approximation may be written :

$$g_{20} \exp[-(t_0 + t'_f/2)/T_2] (t'_f - t'_{th}) = K(t_f - t'_f) \quad (5-7)$$

This, after some rearranging, becomes :

$$\exp[-(t_0 + t'_f/2)/T_2] = (K/g_{20}) (t_f - t'_f) / (t'_f - t'_{th}) \quad (5-8)$$

Figure (5-3) shows  $[(t_f - t'_f) / (t'_f - t'_{th})]$  plotted on a logarithmic scale against  $(t_0 + t'_f/2)$ . The value of  $t'_{th}$  is small with respect to other times, and values have been determined in an approximate fashion from a knowledge of the cavity loss and the ratio of the gains in the two amplifiers. In addition, corrections have been made for the small integral term in equation (5-4) which was dropped in developing equation (5-8). Figure (5-3) shows data obtained for a  $CO_2$ :He gas mixture of 2.8% : 97.2%. The peak gain for the laser tube was 19%, and 6% for the additional amplifier. The cavity loss was approximately 8%. The dotted lines on the figure have slopes corresponding to various values of  $T_2$ . It can be seen that the observed data are well described by an exponential decay, and the value of  $T_2$  so determined is  $11.5 \pm 1 \mu\text{sec}$ . Figure (5-4)



shows similar data obtained for a  $\text{CO}_2:\text{N}_2:\text{He}$  mixture of 3%:3%:94% in the extra amplifier tube. Once more the data fit well to a simple exponential decay with a time,  $T_2$  of  $16 \pm 1$   $\mu\text{sec}$ . These values are in good agreement with the decay times previously measured using the one-amplifier system. Furthermore, the observations are in general agreement with measurements made using direct gain observation techniques (11-15). The data represented in the two figures can be found in Appendix II.

One additional point concerning these measurements is worthy of note. The results obtained with the various gas mixtures in the additional amplifier were checked specifically for interference from time-dependent loss effects in the laser cavity (6,26). This check was made by investigating the effects on  $t_d$  and the laser intensity when the amplifier was operated using appropriate  $\text{N}_2:\text{He}$  mixtures at integrated currents similar to those employed with the  $\text{CO}_2$ -containing mixtures. The results of such observations confirm that time-dependent loss effects had no influence on the reported measurements. However, such effects were observed to significantly disturb the lasing action for sufficiently long delay times between the firing of the amplifier and the oscillator ( $\sim 5$  msec). The  $\text{N}_2:\text{He}$  gas mixture tube used in the above fashion could be employed to investigate thermally-induced loss effects in the laser cavity.

Figure (5-3)

Fall-time of time-dependent gain;  
gas mixture He 97.2% : CO<sub>2</sub> 2.8%

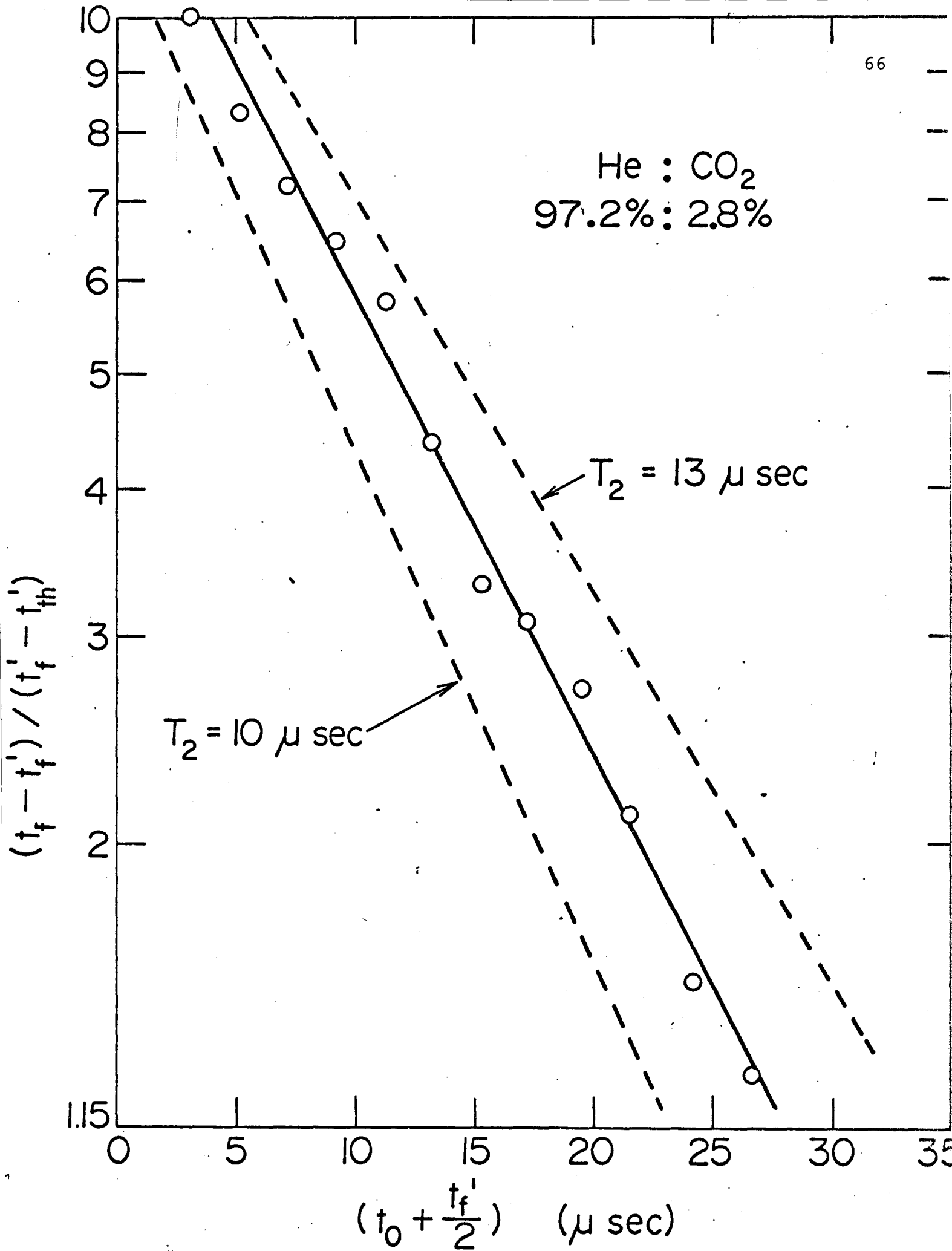
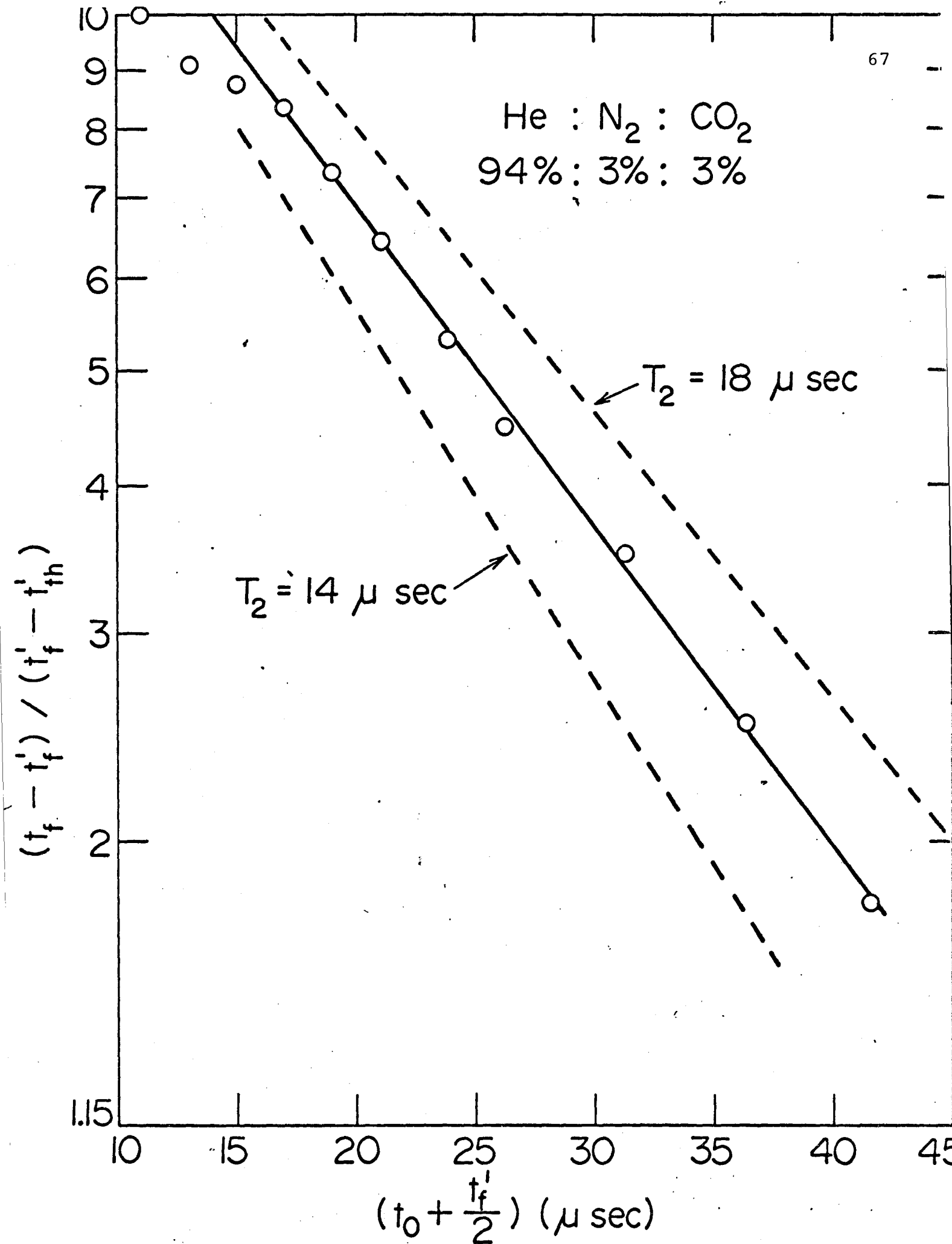


Figure (5-4)

Fall-time of time-dependent gain;  
nitrogen-containing gas mixture  $N_2:CO_2:He = 3\%:3\%:94\%$

He : N<sub>2</sub> : CO<sub>2</sub>  
94% : 3% : 3%





## CHAPTER VI

### CONCLUSIONS AND RECOMMENDATIONS

A relatively simple technique has been demonstrated for obtaining gain and cavity loss parameters in TEA CO<sub>2</sub> lasers to a useful degree of precision. The technique involves the use of the laser output, consequently the intensities to be observed are quite large and radio frequency pick-up problems are minimal. Furthermore, since only time delays are measured, the observations are insensitive to alignment, and any other cause of spurious intensity changes which present problems for direct gain measurement techniques. This technique can be applied in a straightforward fashion to the determination of  $T_1$  and  $T_2$  by variation of the charging voltage, which has been shown to be proportional to the gain under appropriate circumstances. More accurate values of  $T_2$  can be determined using the two-amplifier technique. In addition, both methods can be used to monitor relative changes in the gain or cavity loss. If it is desired to apply the techniques described here to the direct measurement of gain and cavity loss values, it is necessary to calibrate the system. This can be done, as here, by incorporating a variable loss in the laser cavity. Alternatively, the method could be calibrated directly by a one-time direct measurement of the low signal gain of the laser amplifier tube employing a low signal CW CO<sub>2</sub> laser probe.

The results that have been obtained using simple models for the gain and the laser pulse build-up are encouragingly good in view of the complexities of discharges at atmospheric pressure. Observe that one result of the existence of the time-dependent gain is that the threshold for lasing is no longer characterised by the condition that the gain is equal to the loss. For the gain parameters and cavity dimensions employed in the experiments described here, the peak gain must exceed the cavity losses by a factor of almost two before lasing occurs. Another consequence which follows from considerations of build-up times for the laser energy and the time-dependent gain arises in nitrogen-containing gas mixtures. For the nitrogen-containing gas mixture investigated, the gain maximum for high values of normalised charging voltage is such that the laser output pulse occurs well before the gain peak. This reduces the efficiency of the laser and is a contributory cause of the frequently observed double pulsing in such lasers.

The two-amplifier system allows comparison to be made between experimental observations using  $\text{CO}_2$ -containing mixtures and  $\text{He:N}_2$  mixtures operated under similar discharge conditions. This is a direct experimental test for the influence on the lasing action of time-dependent losses in the amplifier tube. This permits the elimination of the influence of such effects on the reported results, and suggests a technique for investigating thermally-induced, time-dependent

loss mechanisms.

The techniques reported in this thesis are all new, no similar work on TEA CO<sub>2</sub> lasers has been attempted before. As is always the case with new techniques, it became obvious that several refinements and improvements are possible. These were not attempted at the time as they required either large-scale equipment modifications, or unnecessary complications to the theory at this early stage. However, they are recorded here for the sake of future researchers.

If large currents are passed through the laser gain tube, bright arcs <sup>(22)</sup> appear and the values of the 1k $\Omega$  resistors change drastically. This limits the maximum current passing through the discharge tube, and hence the peak gain. Even in normal use, the 1k $\Omega$  distributing resistors tend to "age" <sup>(22)</sup>. These effects lead to a somewhat erratic firing of the discharge tube; the gain may change by 10% from pulse to pulse. This is reflected in a variation in the value of  $t_d$  from pulse to pulse, with a consequent lowering of the experimental accuracy. This accuracy can be improved if a stable resistor or resistor configuration is found for the laser gain tube. Work upon these lines is in progress at present. If the charging voltage can be increased to 50 kV, it will be much easier to compare the results from different capacitors, and, of course, a much wider range of experimental data will be obtained.

On the theoretical side, a simple improvement is to

use the accurate values of  $T_2$ , obtained from the two-amplifier system, in the computer program for the single amplifier system. By pinning down one parameter, the fitting process will be made much easier. Another improvement is to take into account the finite width of the current pulse by developing a theory for the pumping of the laser levels. This is a more ambitious step, which may or may not lead to any great improvement in the present fit between theory and experiment.

It is hoped that these conclusions and recommendations, together with the theory and methods outlined earlier in this thesis, will be of value to those wishing to pursue further the investigation of the TEA  $\text{CO}_2$  laser.

## APPENDIX I

### Polishing Method for NaCl

The NaCl discs are bought as rough blanks which must be coarsely ground before a final polish can be applied. The initial grinding is done on sheets of Silicon-Carbide paper stuck on 1/4 inch plate glass to provide a flat surface. Ethanol is used as a lubricant, and the grinding starts on 240 grit paper and proceeds via 320 grit and 400 grit to a final grinding on 600 grit. By this stage, the surface scratches are of order 15  $\mu\text{m}$  deep. The disc is carefully washed in ethanol between each stage. The initial polishing is done using Linde C abrasive powder (1  $\mu\text{m}$  particle size) suspended in ethanol on a Politex Supreme polishing pad. At the completion of this stage, the disc is again carefully washed in ethanol. The procedure so far need only be done once; when repolishing discs affected by humidity, only the final polishing stage need be used.

Two problems are encountered in producing a good final polish. The disc must now be handled only with rubber gloves to prevent skin moisture from attacking the polished surface. A much more serious problem is the condensation of atmospheric moisture in the ethanol. When the ethanol evaporates, patches are left on the polished NaCl surface. This is especially evident on humid days. To overcome this, the ethanol must be

quickly wiped off after the final polish. Three Politex Supreme pads are used for this purpose. The first one carries a mixture of ethanol and Linde A ( $0.3 \mu\text{m}$  particle size). This gives a final surface polish with the deepest scratches of order  $0.3 \mu\text{m}$ . The second pad carries ethanol only and is used to remove the Linde A from the freshly polished surface. The final pad is clean and dry and is used to quickly remove the excess ethanol. The three pads are used in quick succession, and with a little practice, a good clean surface can be obtained. A special holder is used to prevent ethanol reaching the surface which is not being polished. Discs polished by this method were found to have negligible loss when placed in the laser cavity.



## APPENDIX II

### DATA

(a) The first set of data presented here was obtained to determine the relationship between the integrated current and the charging voltage,  $V_c$  (Figure 4-1). The integrated current is determined by photographing the oscilloscope trace and then using a gravimetric technique. The results are accurate to 5-10%. Data for two different capacitors are presented here. The Integrated Current is in arbitrary units.

Capacitor $\mu\text{F}$	Voltage kV	Integrated Current	Remarks
0.01	30	10	Data presented in Figure (4-1)
	27.5	9.05	
	25	8.1	
	22.5	7.3	
	20	6.3	
	18	5.6	
	16	5.2	
	14	4.4	

Capacitor $\mu\text{F}$	Voltage kV	Integrated Current	Remarks
0.005	30	8	With this capacitor, the current pulses are narrower and the noise is more diffi- cult to avoid. Consequently, these measurements are less accurate.
	27.5	7.4	
	25	5.6	
	22.5	5.5	
	20	4.5	
	18	4.2	
	16	3.9	
	14	3.2	

(b) The next set of data was taken to determine the variation of the width of the current pulse with voltage and capacitor. Three different measurements were taken to allow for the changing shape of the pulse. These were (1) full width at half-height, (2) width from peak to half-height, (3) width from peak to 12.5% point. Also measured was the peak current in amps. This is accurate to better than 10%. The widths are all accurate to about 10%; the lower voltage measurements are the more erratic. Two different gas mixtures were used.



Gas Mixture	Capacitor $\mu\text{F}$	Voltage kV	Current Peak, Amps	(1) $\mu\text{S}$	(2) $\mu\text{S}$	(3) $\mu\text{S}$
97.2% He:	0.02	20	640	0.52	0.3	0.75
		18	520	0.58	0.32	0.9
		16	350	0.62	0.38	1.4
2.8% CO <sub>2</sub>	0.01	30	1150	0.32	0.15	0.25
		26	900	0.35	0.16	0.32
		22	640	0.36	0.18	0.45
		20	520	0.38	0.20	0.5
		18	380	0.4	0.24	0.7
		16	270	0.5	0.28	0.9
		14	160	0.6		1.5
	0.005	30	900	0.23	0.13	0.2
		26	720	0.25	0.14	0.22
		22	500	0.25	0.15	0.32
		20	400	0.27	0.15	0.4
		18	290	0.3	0.18	0.5
		16	220	0.38	0.22	0.7
		14		too unstable		
0.0025	0.0025	30	600	0.19	0.09	0.15
		26	440	0.2	0.1	0.17
		22	320	0.21	0.11	0.23

		20	260	0.24	0.12	0.35
		18	200	0.25	0.15	0.42
94.4% He:	0.01	30	920	.35	.18	.35
		26	720	.35	.20	.52
5.6% CO <sub>2</sub>		22	460	.38	.23	.65
		20	350	.44	.28	.88
		18	240	.50	.3	1.2
		16	too unstable			
	0.005	30	740	.25	.13	.25
		26	540	.27	.15	.32
		22	350	.3	.16	.5
		20	270	.35	.20	.64
		18	180	.5	.3	.8
		16	120	.6	.40	1.0
	0.0025	30	500	.20	.10	.2
		26	350	.20	.10	.25
		22	230	.36	.16	.4
		20	180		.3	.5
		18	130			.6
		16	80			

Some of this data is used in Figure (4-2).

(c) This set of data represents the bulk of the work done on the laser pulse delay times,  $t_d$ . Three different capacitors were used, and several different gas mixtures. The variable loss unit was set at zero for these measurements. Each value for  $t_d$  is the average of several measurements. The accuracy is indicated approximately in the error column.

Gas Mixture 97.2% He : 2.8% CO <sub>2</sub>				
Capacitor	Voltage	$t_d$	Error	Remarks
$\mu\text{F}$	kV	$\mu\text{sec.}$	$\mu\text{sec.}$	
0.01	30	1.18	$\pm 0.04$	
	26	1.24		
	22	1.34		
	20	1.4	$\pm 0.06$	
	18	1.52		
	16	1.72		
0.005	30	1.7	$\pm < 0.1$	
	26	1.8		
	24	2.0		
	22	2.2		
	20	2.35		
	18	2.65	$\sim \pm 0.1$	
	16	3.1		

0.0025	30	2.7	± 0.2
	28	2.8	
	26	3.25	
	24	3.8	± 0.3
	22	4.7	± 0.4
	20	5.6	
	18	7	± 1.0
	17	8	
	16	does not lase	

This completes the set of data giving the relation found in Figure (4-3). The data used in Figure (4-4) is given below:

<u>Gas Mixture 94.4% He : 5.6% CO<sub>2</sub></u>				
Capacitor	Voltage	t <sub>d</sub>	Error	Remarks
μF	kV	μsec.	μsec.	
0.01	30	0.95		
	26	1.00		
	24	1.04		
	22	1.12		
	20	1.2	± 0.05	
	18	1.4		
	16	1.8		very erratic

0.005	30	1.48	$\pm 0.1$
	26	1.64	
	22	1.8	
	20	2.0	
	18	2.3	
	16	3.0	$- 0.2 + 0.5$
0.0025	30	2.45	$\pm 0.2$
	28	2.6	
	26	2.9	$\pm 0.3$
	24	3.15	
	22	3.65	$\pm 0.3$
	20	4.5	
	18	6	

A further set of data was taken for a He:CO<sub>2</sub> gas mixture containing only 1.4% CO<sub>2</sub>.

Capacitor	Voltage	$t_d$	Error	Remarks
$\mu\text{F}$	kV	$\mu\text{sec.}$	$\mu\text{sec.}$	
0.01	30	1.66	$\pm 0.02$	
	28	1.7		
	26	1.8		
	24	2.0	$\pm 0.05$	
	22	2.2		

	20	2.35	
	18	2.55	
	16	2.9	$\pm 0.1$
0.005	30	2.45	
	28	2.7	$\pm 0.1$
	26	3.1	
	24	3.5	
	22	4.25	$\pm 0.2$
	20	5.2	
	18	~8	
	16	does not lase	
0.0025	30	4.4	$\pm 0.2$
	28	5.3	
	26	7.5	
	25	9	$\pm 1.0$

The final set of data in this section concerns the nitrogen-containing gas mixture.

Gas Mixture : 3% N<sub>2</sub> : 3% CO<sub>2</sub> : 94% He

---

Capacitor	Voltage	t <sub>d</sub>	Remarks
μF	kV	μsec.	
0.01	30	1.2	
	26	1.34	
	22	1.52	
	20	1.64	
	18	1.8	
	16	2.2	
0.005	30	1.76	
	26	1.8	
	22	1.9	
	20	2.05	
	18	2.35	
	16	2.8	
0.0025	30	2.35	
	26	2.6	
	22	2.9	
	20	3.3	
	18	3.8	
	16	4.6	
	14	~7	Erratic

0.001	30	4.4	All the measurements with this capacitor are very inaccurate. $t_d$ is very sensitive to small changes in gain or loss.
	26	5	
	22	6.5	
	20	8	
	18	10.4	
	17	12	
	15	does not lase	

(d) The next set of data was taken using the variable loss unit. The data is plotted in Figure (4-5).

Gas Mixture 97.2% He : 2.8% CO<sub>2</sub>

Capacitor $\mu\text{F}$	Voltage kV	Inserted Loss %	$t_d$ $\mu\text{sec.}$	Remarks
0.01	30	0	1.2	Variable Loss unit set at Brewster's angle.
	26		1.3	
	22		1.42	
	18		1.68	
	16		1.86	
0.005	30	0	1.8	Each value of $t_d$ is the average of several measurements.
	26		2.0	
	22		2.45	
	18		3.1	
	16		3.65	



0.0025	30	0	3.1	
	26		3.7	
	22		5.5	
	20		7-8	
	19			does not lase
0.01	30	3%	1.44	
	26		1.5	
	22		1.68	
	20		1.8	
	18		2.0	
	16		2.25	
0.005	30	3%	2.15	
	28		2.3	
	26		2.5	
	24		2.8	$t_d$ erratic at
	22		3.2	these voltages
Capacitor	Voltage	Inserted	$t_d$	Remarks
$\mu\text{F}$	kV	Loss %	$\mu\text{sec.}$	
0.005	20	3%	3.8	
	18		4.5	
	16			does not lase

0.01	30	10%	1.92	
	28		2.0	
	26		2.2	
	24		2.5	
	22		2.7	
	20		3	
	18		4	
	16			does not lase
0.01	30	12.5%	2.5	
	28		2.8	
	26		3.1	
	24		4.25	
	22			does not lase
0.01	30	13.5%	3.2	
	28		3.75	
	26			does not lase

(e) The final set of data is that used in Figures (5-3) and (5-4). The two amplifier tubes are fixed with a time-delay of  $t_0$  between them.  $\Delta t$  is the change in the time-delay,  $t_d$ , of the laser pulse due to the effect of the short amplifier tube.

Gas Mixture : 97.2% He : 2.8% CO<sub>2</sub> (Short Tube)

$t_0$	$t_d$	$\Delta t$
$\mu\text{sec.}$	$\mu\text{sec.}$	$\mu\text{sec.}$
30	3.4	<0.1
27.5		0.24
25		0.25
22.5		0.3
20		0.4
18		0.5
16		0.55
14		0.6
12		0.75
10		0.92
8		1.0
6		1.1
4		1.2
2		1.35

Gas Mixture : 3% N<sub>2</sub> : 3% CO<sub>2</sub> : 94% He (Short Tube)

50	3.4	0.1
45		0.2
40		0.4
35		0.55
30		0.7

25	0.8
22.5	0.95
20	1.1
18	1.2
16	1.3
14	1.4
12	1.4
10	1.5
8	1.55

## REFERENCES

1. A. J. Beaulieu, "Transversely Excited Atmospheric Pressure CO<sub>2</sub> Lasers", Applied Physics Letters, 16, 504-5, (1970).
2. A. K. Laflamme, "Double Discharge Excitation for Atmospheric Pressure CO<sub>2</sub> Lasers", Review of Scientific Instruments, 41, 1578-81, (1970).
3. H. M. Lamberton and P. R. Pearson, "Improved Excitation Techniques for Atmospheric Pressure CO<sub>2</sub> Lasers", Electronic Letters, 7, 141-142, (1971).
4. D. C. Johnson, "Excitation of an Atmospheric-Pressure CO<sub>2</sub>-N<sub>2</sub>-He Laser by Capacitor Discharges", IEEE Journal of Quantum Electronics, QE-7, 185-9, (1971).
5. L. J. Denes and O. Farish, "High-pressure pulsed CO<sub>2</sub> laser with uniform excitation", Electronic Letters, 7, 337-8, (1971).
6. R. Fortin, M. Gravel and R. Temblay, "Helical TEA-CO<sub>2</sub> Lasers", Canadian J. Physics, 49, 1783-93, (1971).
7. J. A. Beaulieu, "High Peak Power Gas Lasers", Proceedings of the IEEE, 59, 667-73, (1971).
8. R. C. Crafer, A. F. Gibson, M. J. Kent and M. F. Kimmit, "Time-Dependent processes in CO<sub>2</sub> laser amplifiers", J. Physics D., Ser 2 Vol 2, 183-95, (1969).
9. B. K. Garside, E. A. Ballik and J. Reid, "Pulse Delays in TEA CO<sub>2</sub> Lasers", to be published in J. Appl. Phys., May 1972.

10. J. Reid, B. K. Garside and E. A. Ballik, "Effects of time delayed Amplification in TEA CO<sub>2</sub> Lasers", to be published in IEEE J. Quan. Electronics, May 1972.
11. A. M. Robinson, "Afterglow gain measurements in CO<sub>2</sub>-He-N<sub>2</sub> mixture at pressures up to one atmosphere", Canadian J. Physics, 48, 1996-2001, (1970).
12. A. M. Robinson, "High Gain Pulsed CO<sub>2</sub> Transverse Discharge Amplifier", Physics Letters, 35A, 47-8, (1971).
13. D. C. Smith and A. J. DeMaria, "Parametric Behaviour of the Atmospheric Pressure Pulsed CO<sub>2</sub> Laser", J. Applied Physics, 41, 5212-4, (1970).
14. A. M. Robinson, "Spatial Resolution of gain in CO<sub>2</sub> Transversely Excited Pulsed Discharge", J. Applied Physics, 42, 4098-4104, (1971).
15. MIT Quarterly Progress Report No. 102, "Electrodynamics of Media", 59-64, (1971).
16. J. Tulip, "Gain Saturation of the CO<sub>2</sub> Laser", IEEE J. Quantum Electronics, QE-6, 206, (1970).
17. C. B. Moore, R. E. Wood, Bei-Lok Hu and J. J. Yardley, "Vibrational Energy Transfer in CO<sub>2</sub> Lasers", J. Chemical Physics, 46, 4222-31, (1967).
18. B. K. Garside, "Mode Spectra in Ring and Normal Lasers", IEEE J. Quantum Electronics, QE-4, 940-8, (1968).
19. A. F. Gibson, M. F. Kimmitt and A. C. Walker, "Photon Drag in Germanium", Applied Physics Letters, 17, 75-77, (1970).

20. J. Gilbert and J. L. Lachambre, "Self-locking of modes in a high pressure CO<sub>2</sub> laser with transverse pulse excitation", Applied Physics Letters, 18, 187-9, (1971).
21. A. Crocker and H. M. Lamberton, "Output Pulse Characteristics and Self-Mode Locking of Atmospheric Pressure CO<sub>2</sub> Lasers", Electronic Letters, 7, 272-273, (1971).
22. E. A. Ballik, B. K. Garside and J. Reid, "Properties of TEA CO<sub>2</sub> Lasers", Research Report presented to Defence Research Establishment, Valcartier, (1971).
23. R. Fortin, "Preliminary Measurements of a Transversely Excited Atmospheric Pressure CO<sub>2</sub> Laser", Canadian J. Physics, 49, 257-64, (1970).
24. W. A. Rosser, Jr., and E. T. Gerry, "De-excitation of Vibrationally Excited CO<sub>2</sub> by collisions with He, O<sub>2</sub> and H<sub>2</sub>O", J. Chem. Phys., 51, 2286-7, (1969) (and cited references).
25. P. K. Cheo, "Relaxation of CO<sub>2</sub> Laser Levels by Collisions with Foreign Gases", IEEE J. Quantum Electronics, QE-4, 587-93, (1968).
26. G. Otis and R. Tremblay, "Time-Dependent lensing effects in TEA CO<sub>2</sub> lasers", Optics Communications, 3, 418-420, (1971).